

MULTISCALE METHODS FOR WAVE PROPAGATION IN MATERIALS WITH SIGN-CHANGING COEFFICIENTS*

ERIC T. CHUNG[†], PATRICK CIARLET JR.[‡], XINGGUANG JIN[§], AND CHANGQING YE[¶]

Abstract. From a mathematical perspective, the extraordinary properties of metamaterials are often reflected in the coefficients of the governing partial differential equations (PDEs). These coefficients may fall outside the assumptions of classical theory, particularly when the effective dielectric permittivity and/or magnetic permeability are negative. This situation can transform a coercive operator into a non-coercive one, potentially leading to ill-posedness. In this paper, we utilize the Constraint Energy Minimizing Generalized Multiscale Finite Element Method (CEM-GMsFEM), specifically designed for time-harmonic electromagnetic wave problems, where the construction of auxiliary spaces in the original CEM-GMsFEM is tailored to accommodate the sign-changing setting. Based on the framework of T-coercivity theory and resolution conditions, we establish the inf-sup stability and provide an a priori error estimate for the proposed method. The numerical results demonstrate the effectiveness and robustness of our approach in handling such sophisticated coefficient profiles.

Key words. Negative index materials, multiscale potential, multiscale finite element method

AMS subject classifications. 65M12, 65M15, 65N30

1. Introduction. Metamaterials have revolutionized the human understanding of materials science and engineering. Typically, metamaterials are engineered by arranging functional cells in a periodic structure, resulting in effective properties that exhibit behaviors markedly different from those of conventional materials. Veselago, a Soviet physicist, conceived the concept of negative refractive indices in 1967 [23]. Intuitively, light passing through these types of materials bends in the opposite direction compared to conventional materials. Much later, Pendry et al. proposed a viable design for experimental realization [19], and Shelby, Smith, and Schultz [22] achieved the first successful fabrication in 2001. Another significant driving force behind the study of Negative-Index Metamaterials (NIM) was the potential for perfect lensing, which could surpass the diffraction limit of conventional lenses [20]. Given the considerable application potential associated with fabrication, in-silico simulations have become crucial for the design and optimization of NIMs.

From a mathematical perspective, the extraordinary properties of metamaterials are often reflected in the coefficients of the governing partial differential equations (PDEs), which may deviate from the assumptions of classical theory. Consider NIMs, where the electronic permittivity and magnetic permeability are both negative. When NIMs are embedded in a conventional medium, i.e. air, the governing PDEs exhibit coefficients that change sign globally. In a time-harmonic regime, this can transform a coercive operator into a non-coercive one, potentially leading to ill-

*Submitted to the editors DATE.

Funding: The research of Eric Chung is partially supported by the Hong Kong RGC General Research Fund (Projects: 14305624 and 14305423).

[†]Department of Mathematics, The Chinese University of Hong Kong, Hong Kong (tschung@math.cuhk.edu.hk).

[‡]POEMS, CNRS, INRIA, ENSTA Paris, Institut Polytechnique de Paris, 91120 Palaiseau, France (patrick.ciarlet@ensta.fr).

[§]Corresponding author. Department of Mathematics, The Chinese University of Hong Kong, Hong Kong (xgjin@math.cuhk.edu.hk).

[¶]Department of Mathematics, The Chinese University of Hong Kong, Hong Kong (Ye.Changqing@outlook.com).

posedness. This scenario poses significant challenges for both the theoretical analysis and numerical simulations. Over the past two decades, mathematicians have made considerable progress in understanding the rich insights of these PDEs, laying a robust foundation for numerical investigations. In particular, the T-coercivity theory introduced by Bonnet-Ben Dhia, Ciarlet, and Zwölf in their work [3] is of particular importance, which establishes a unified framework for the well-posedness of PDEs with sign-changing coefficients. The key idea behind T-coercivity is to devise a bijective map \mathcal{T} that enables the inf-sup (Banach–Necas–Babuška) condition to hold trivially. The construction of \mathcal{T} is based only on the geometric information of the interfaces that separate the subdomains with different signs of the coefficient. The main statement of the T-coercivity theory is that if the contrast ratio between the negative and positive coefficients is sufficiently large, then the model problem becomes well-posed. In [4], the sharpest condition of the contrast ratio was derived to ensure well-posedness on certain simple interface problems. Further extensions of the T-coercivity theory encompass Helmholtz-like problems [13], time-harmonic Maxwell equations [6, 5], eigenvalue problems [7], and mixed problems [2].

The magnificent phenomena of NIMs are usually attributed to their interaction with common materials. Consequently, heterogeneity is a significant feature in meta-material numerical simulations and should therefore be carefully addressed. Multiscale computational methods, which aim to capture the small-scale information of solutions due to heterogeneity at a reduced computational cost, are particularly well-suited for this task. Pioneered by Hou and Wu in [14], the methodology of incorporating model information into the construction of finite element spaces, coined as MsFEMs, has garnered significant attention. The evolution version, GMsFEMs, leverages spectral decomposition to perform dimension reduction for the online space, exhibiting superior performance when dealing with high-contrast and channel-like coefficient profiles [12]. The first construction of multiscale bases capable of achieving the theoretically optimal approximation property for general rough coefficients was credited to Målqvist and Peterseim in their celebrating work [18]. The combination of GMsFEMs and LOD led to the development of a CEM-GMsFEM by Chung, Efendiev, and Leung in [11], where “CEM” is the acronym for “Constraint Energy Minimizing”. Constrained Energy Minimizing Generalized Multiscale Finite Element Method (CEM-GMsFEM), which demonstrates superior performance in high-contrast problems, has been successfully applied to various partial differential equations arising from practical applications [17, 29]. Constructing multiscale bases in CEM-GMsFEMs involves two steps: solving engineered generalized eigenvalue problems to obtain auxiliary spaces and localizing multiscale bases in a relaxed or constrained manner. Several primary successful results on Laplace-type PDEs with sign-changing coefficients have been achieved in [27] through the tailored construction of auxiliary spaces to accommodate the sign-changing setting.

Despite these advancements, the current multiscale methods are still inadequate for NIM simulations, especially for electromagnetic wave problems. This claim is based on the following observed facts: (1) the current multiscale methods are primarily designed for Laplacian-type elliptic PDEs [27, 8]. At the same time, electromagnetic wave simulations involve the more complex double-curl operator. (2) Although with several numerical demonstrations, the high wave number regime remains challenging; (3) the sign-changing coefficients and the non-coercive nature undermine the numerical analysis. This paper aims to address the scalar electromagnetic wave equation in the time-frequency domain by developing GEM-GMsFEMs for NIM simulations. Multiscale computational methods are initially designed to address heterogeneity in

elliptic PDEs. However, accuracy can be compromised by high contrast coefficients in the PDEs. In the analysis section, we establish a resolution condition that aids in addressing the term involving the wave number. This condition allows us to absorb the wavenumber into the Laplacian term, facilitating the formulation of the inf-sup condition for both global and multiscale problems, thereby ensuring their well-posedness. The stability of GEM-GMsFEMs in the high contrast regime relies on auxiliary spaces, which are constructed by solving generalized eigenvalue problems. The well-posedness of CEM-GMsFEM is in fact guaranteed by utilizing the abstract framework of T-coercivity theory [1] to construct the inf-sup conditions. As emphasized earlier, CEM-GMsFEMs remain unexplored for conventional electromagnetic wave simulations. These observations motivate us to develop a novel multiscale method, starting with common electromagnetic wave simulations and progressing to NIM simulations.

To the best of our knowledge, efforts to apply multiscale computational methods to electromagnetic wave problems are currently scarce. An exception can be found in the work by Chung and Ciarlet in [10], where they employed the staggered discontinuous Galerkin method [15, 9]. Note that contrast ratios play a significant role in the T-coercivity theory to assess the well-posedness of the model problem. In comparison, the proposed method presented in this paper is more general, as it can handle a broader range of coefficient profiles, including those with high contrast ratios.

This paper is organized as follows. In section 2, we introduce the model problem and present the T-coercivity theory. The construction of multiscale bases in the proposed method is detailed in section 3. To validate the performance of the proposed method, section 5 presents numerical experiments conducted on four different models. All theoretical analysis for the proposed method is gathered in section 4. Finally, in section 6, we conclude the paper.

2. Preliminaries. Let $\Omega \subset \mathbb{R}^2$ be an open bounded domain, which can be split into two subdomains Ω^+ and Ω^- without overlapping. Here, we adopt the notations for all quantities $\sigma, \sigma^{-1}, c, c^{-1} \in L^\infty(\Omega)$ defined on Ω such that

$$\begin{cases} x \in \Omega^+, \sigma(x) > 0 : \sigma_{\max}^+ = \sup \sigma(x), \sigma_{\min}^+ = \inf \sigma(x). \\ x \in \Omega^-, \sigma(x) < 0 : \sigma_{\max}^- = \sup |\sigma(x)|, \sigma_{\min}^- = \inf |\sigma(x)|. \end{cases}$$

We consider the following Helmholtz-like equation with sign-changing coefficients σ and c in the bounded space domain $\Omega \subset \mathbb{R}^2$ imposed by homogeneous boundary conditions:

$$(2.1) \quad -\nabla \cdot (\sigma \nabla u) - k^2 cu = f,$$

where $k \in \mathbb{R}$ is a positive wavenumber, $f \in L^2(\Omega)$ represents a harmonic source. Redefine the Sobolev space $V = H_0^1(\Omega)$ and write the boundary value problem (2.1) in a variational form: find a solution $u \in V$ such that for all $v \in V$,

$$(2.2) \quad \int_{\Omega} \sigma \nabla u \cdot \nabla v \, dx - k^2 \int_{\Omega} cuv \, dx = \int_{\Omega} fv \, dx, \quad \forall v \in V,$$

To simplify the notations, the sesquilinear form $\mathcal{B} : V \times V \rightarrow \mathbb{R}$ satisfies

$$(2.3) \quad \mathcal{B}(u, v) := (\sigma \nabla u, \nabla v) - k^2 (cu, v),$$

where $(u, v) = \int_{\Omega} uv \, dx$. Then we rewrite (2.2) in the following

$$(2.4) \quad \mathcal{B}(u, v) = (f, v) = l(v).$$

The weak form (2.4) is well-posed if and only if $l(v) = 0$ implies $u = 0$. It is convenient to introduce a notation for a norm as $\|v\|_{\bar{a},\omega} := (\int_{\omega} |\sigma| |\nabla v|^2 dx)^{1/2}$, where ω is a subdomain of Ω . Moreover, we abbreviate $\|\cdot\|_{\bar{a},\Omega}$ as $\|\cdot\|_{\bar{a}}$. Based on the definition of T-coercivity: If there exists a bijective operator $\mathcal{T} : V \rightarrow V$, such that $\forall v \in V$, $\exists \gamma > 0$, a bilinear form a satisfies $|a(v, \mathcal{T}v)| \geq \gamma \|v\|_{\bar{a}}^2$. If we split form \mathcal{B} as $\mathcal{B} = a + b$ where $a = (\sigma \nabla u, \nabla v)$ and $b = -k^2(cu, v)$, then the T-coercivity of the bilinear form $a(v, \mathcal{T}v)$ can be obtained under the sufficiently large high-contrast ratio $\Upsilon = \frac{\sigma_{\min}^+}{\sigma_{\max}}$ in [27], and the construction of \mathcal{T} is given by

$$(2.5) \quad \mathcal{T}v = \begin{cases} v_1, & \text{in } \Omega^+, \\ -v_2 + 2\mathcal{R}v_1, & \text{in } \Omega^-, \end{cases}$$

where

$$(2.6) \quad v = \begin{cases} v_1, & \text{in } \Omega^+, \\ v_2, & \text{in } \Omega^-. \end{cases}$$

Here, we assume the existence of a bounded map $\mathcal{R} : V^+ \rightarrow V^-$ with $\mathcal{R}v|_{\Gamma} = v|_{\Gamma}$ in the sense of Sobolev traces, and the second term $b(\cdot, \mathcal{T}\cdot)$ is a compact perturbation due to the compacting embedding theorem [3].

As is shown in Figure 1, let \mathcal{K}_H be a standard quadrilateralization of the domain Ω with the mesh size H . We refer to this partition as coarse grids, and the produced elements as the coarse elements. Each coarse element $K \in \mathcal{K}_H$ is further partitioned into a union of connected fine grid blocks. We denote the fine-grid partition as \mathcal{K}_h with $h > 0$ being the fine grid size. For each $K_i \in \mathcal{K}_H$ with $1 \leq i \leq N$, N is the number of coarse elements. we define an oversampled domain $K_i^m (m \geq 1)$ in the following

$$K_i^m := \text{int} \left\{ \bigcup_{K \in \mathcal{K}_H} \{ \overline{K_i^{m-1}} \cap \overline{K} \neq \emptyset \} \cup \overline{K_i^{m-1}} \right\},$$

where $\text{int}(S)$ and \overline{S} represent the interior and the closure of a set S , and the initial value $K_i^0 = K_i$ for each element.

3. CEM-GMsFEM. To facilitate the construction of the eigenvalue problems and the subsequent analysis, we can assume that the value of c in the equation (2.1) is proportional to σ . In the original CEM-GMsFEM, a generalized eigenvalue problem,

$$(3.1) \quad \begin{aligned} & \text{find } \lambda \in \mathbb{R} \text{ and } v \in H^1(K_i) \setminus \{0\} \\ & \text{s.t. } \forall w \in H^1(K_i), \int_{K_i} \sigma \nabla v \cdot \nabla w \, dx = \lambda \int_{K_i} \mu_{\text{msh}} \text{diam}(K_i)^{-2} c v w \, dx, \end{aligned}$$

is solved on each coarse element K_i , where μ_{msh} is a generic positive constant that depends on the mesh quality. Then the local auxiliary space V_i^{aux} is formed by collecting leading eigenvectors. However, recalling that σ is not uniformly positive, the left-hand bilinear form in (3.1) is not positive semidefinite, and similarly, the right-hand bilinear form in (3.1) is not positive definite. Then, determining leading eigenvectors via (3.1) is problematic since the eigenvalues could be negative. To address this issue, we instead construct the following generalized eigenvalue problem

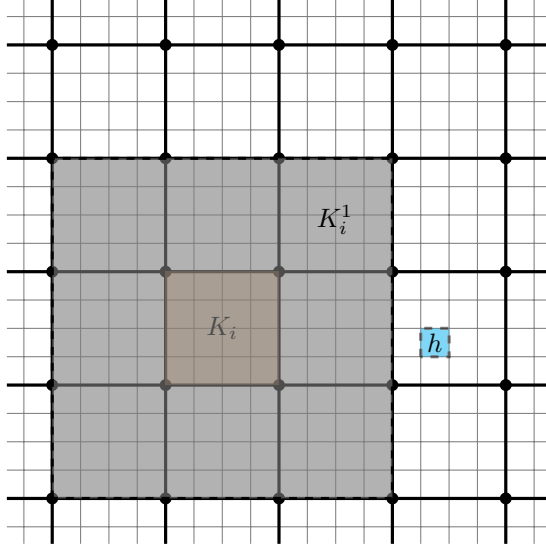


Fig. 1: An illustration of the two-scale mesh, a fine element h , a coarse element K_i and its oversampling coarse element K_i^m with the oversampling layer $m = 1$.

on each K_i , which forms the first step of the proposed method:

$$(3.2) \quad \begin{aligned} & \text{find } \lambda \in \mathbb{R} \text{ and } v \in H^1(K_i) \setminus \{0\} \\ & \text{s.t. } \forall w \in H^1(K_i), \int_{K_i} |\sigma| \nabla v \cdot \nabla w \, dx = \lambda \int_{K_i} \mu_{\text{msh}} \text{diam}(K_i)^{-2} |c| v w \, dx. \end{aligned}$$

Upon solving the l_* leading eigenvectors in (3.2), denoted as ψ_i^j with $1 \leq j \leq l_*$, we can construct the local auxiliary space $V_i^{\text{aux}} \subset L^2(K_i)$ as $\text{span}\{\psi_i^j\}$ for $1 \leq i \leq N$. The global auxiliary space $V^{\text{aux}} \subset L^2(\Omega)$ is defined as $V^{\text{aux}} = \bigoplus_{i=1}^{N_{\text{elem}}} V_i^{\text{aux}}$, where $V_i^{\text{aux}} \subset L^2(\Omega)$ is the space by performing zero-extension of functions in V_i^{aux} . We introduce several notations for future reference. Let μ be a function in $L^\infty(\Omega)$ satisfying

$$\mu|_{K_i} = \mu_{\text{msh}} \text{diam}(K_i)^{-2} c|_{K_i}$$

for all $K_i \in \mathcal{K}_H$. Next, for a subdomain ω in Ω , we define two bilinear forms:

$$a(v, w)_\omega := \int_\omega \sigma \nabla v \cdot \nabla w \, dx \text{ and } s(v, w)_\omega := \int_\omega \mu v w \, dx.$$

Similarly to the definition of $\|v\|_{\tilde{a}, \omega}$, we define $\|v\|_{\tilde{s}, \omega}$ as $(\int_\omega |\mu| |v|^2 \, dx)^{1/2}$. Again, we drop the subscript ω if $\omega = \Omega$. Additionally, we define the orthogonal projection operator $\pi: L^2(\Omega) \rightarrow L^2(\Omega)$ under the norm $\|\cdot\|_{\tilde{s}}$, with $V^{\text{aux}} = \text{im } \pi$. The following Lemma 3.1 demonstrates the properties of the global projection π , which will be frequently utilized in the analysis. Its proof is a straightforward application of the properties of eigenspace expansions. We also use the shorthand notation V_i^m as $H_0^1(K_i^m)$, and we always implicitly identify V_i^m as a subspace of V . The functions in V^{aux} may not be continuous in Ω , and thus V^{aux} cannot be used as a finite element space. In the next section, subsection 3.1, we will construct a multiscale basis $\phi_{i,m}^j$ in

V_i^m , corresponding to ψ_i^j in V_i^{aux} , which is obtained in equation (3.2). Before that, we will list a collection of estimates related to the \mathcal{T} operator, which will help pave the way for proving the well-posedness of the global multiscale basis function in equation (3.11).

LEMMA 3.1. *In each $K_i \in \mathcal{K}_H$, for all $v \in H^1(K_i)$,*

$$(3.3) \quad \|v - \pi_i v\|_{\bar{s}, K_i}^2 \leq \frac{\|v\|_{\bar{a}, K_i}^2}{\lambda_i^{l_*+1}} \leq \Lambda^{-1} \|v\|_{\bar{a}, K_i}^2,$$

where $\Lambda = \min_{1 \leq i \leq N} \lambda_i^{l_*+1}$, and

$$(3.4) \quad \|\pi_j v\|_{\bar{s}, K_i}^2 = \|v\|_{\bar{s}, K_i}^2 - \|v - \pi_j v\|_{\bar{s}, K_i}^2 \leq \|v\|_{\bar{s}, K_i}^2.$$

LEMMA 3.2. *It holds that for any $v \in V$, \mathcal{T} is the operator defined in (2.5),*

$$(3.5) \quad a(v, \mathcal{T}v) \geq \left(1 - \|\mathcal{R}\|_1 / \sqrt{\Upsilon}\right) \|v\|_{\bar{a}}^2,$$

$$(3.6) \quad s(\pi v, \pi \mathcal{T}v) \geq \left(1 - \|\mathcal{R}\|_0 / \sqrt{\Upsilon}\right) \|\mathcal{P}_H v\|_{\bar{s}}^2 - \Lambda^{-1} \|\mathcal{R}\|_0 / \sqrt{\Upsilon} \|v\|_{\bar{a}}^2,$$

$$(3.7) \quad \|\mathcal{T}v\|_{\bar{a}} \leq \max \left\{ \left(1 + 8\|\mathcal{R}\|_1^2 / \Upsilon\right)^{1/2}, \sqrt{2} \right\} \|v\|_{\bar{a}},$$

$$(3.8) \quad \|\mathcal{T}v\|_{\bar{s}} \leq \max \left\{ \left(1 + 8\|\mathcal{R}\|_0^2 / \Upsilon\right)^{1/2}, \sqrt{2} \right\} \|v\|_{\bar{s}},$$

where for any $w \in V(\Omega^+)$,

$$(3.9) \quad \|\nabla \mathcal{R}w\|_{\Omega^-} \leq \|\mathcal{R}\|_1 \|\nabla w\|_{\Omega^-} \quad \text{and} \quad \|\mathcal{R}w\|_{\Omega^-} \leq \|\mathcal{R}\|_0 \|w\|_{\Omega^+}.$$

Proof. The detailed proof can be found in [27]. To facilitate the analysis, we introduce the following notations for constants that are from (3.5)–(3.8):

$$C_0 := \max \left\{ \left(1 + 8\|\mathcal{R}\|_1^2 / \Upsilon\right)^{1/2}, \sqrt{2} \right\},$$

$$C_1 := \max \left\{ \left(1 + 8\|\mathcal{R}\|_0^2 / \Upsilon\right)^{1/2}, \sqrt{2} \right\},$$

$$C_2 := \min \left\{ 1 - \|\mathcal{R}\|_1 / \sqrt{\Upsilon} - \Lambda^{-1} \|\mathcal{R}\|_1 / \sqrt{\Upsilon}, 1 - \|\mathcal{R}\|_0 / \sqrt{\Upsilon} \right\}.$$

We can see that C_0 , C_1 , and C_2 can all be bounded from above and below, provided that Υ is sufficiently large and Λ^{-1} is sufficiently small. \square

3.1. Multiscale basis functions. For each coarse element $K_i \in \mathcal{K}_H$ and its oversampling domain $K_i^m \subset \Omega$ by enlarging K_i for m coarse grid layers, we define the multiscale basis function $\phi_{i,m}^j \in V_0(K_i^m)$, find $\phi_{i,m}^j \in V_0(K_i^m)$ such that

$$(3.10) \quad \mathcal{B}(\phi_{i,m}^j, w) + s(\pi \phi_{i,m}^j, \pi w) = s(\psi_i^j, \pi w), \quad \forall w \in V_0(K_i^m),$$

where $V_0(K_i^m)$ is the subspace of $V(K_i^m)$ with zero trace on ∂K_i^m and $V(K_i^m)$ is the restriction of V in K_i^m . Now, our multiscale finite element space V_{ms} can be defined by solving an variational problem (3.10)

$$V_{\text{ms}} = \text{span} \left\{ \phi_{i,m}^j \mid 1 \leq j \leq l_*, 1 \leq i \leq N \right\}.$$

The global multiscale basis function $\phi_i^j \in V$ is defined in a similar way,

$$(3.11) \quad \mathcal{B}(\phi_i^j, w) + s(\pi\phi_i^j, \pi w) = s(\psi_i^j, \pi w), \quad \forall w \in V(K_i),$$

Thereby, the global multiscale finite element space V_{glo} is defined by

$$V_{\text{glo}} = \text{span}\left\{\phi_i^j \mid 1 \leq j \leq l_*, 1 \leq i \leq N\right\}.$$

The existence of the above two variational problems will be shown in the analysis part. In the following, we need to find the approximated solution of (2.4): Find $u_{\text{ms}} \in V_{\text{ms}}$ such that

$$(3.12) \quad \mathcal{B}(u_{\text{ms}}, w) = (f, w), \quad \forall w \in V_{\text{ms}}.$$

LEMMA 3.3. *For any $v_{\text{glo}} \in V_{\text{glo}}$ and $w \in \tilde{V}$, it holds $\mathcal{B}(v_{\text{glo}}, w) = 0$. If $w \in V$ and $\mathcal{B}(v_{\text{glo}}, w) = 0$ holds for any v_{glo} , then $w \in \tilde{V}$, where $\tilde{V} = \{v \in V \mid \pi(v) = 0\}$.*

Proof. For any $v_{\text{glo}} \in V_{\text{glo}}$, by using the fact in (3.11), it is easy to obtain the first argument. For the second argument, $\forall w \in V$, we have $\mathcal{B}(v_{\text{glo}}, w) = 0$. By using the contradiction and mimicking the proof steps in [27], we can obtain that $\pi w = 0$, then $w \in \tilde{V}$. \square

4. Analysis.

LEMMA 4.1. *If the mesh size H , the wavenumber k satisfies the resolution condition such that*

$$(4.1) \quad C_1 \mu_{\text{msh}}^{-1} k^2 H^2 \leq C_* \Lambda,$$

where C_1 is the constant related to \tilde{s} norm under T -coercivity in (3.8) and $C_* < 1$ is a constant. Under the resolution condition, \mathcal{T}_H is the operator on \tilde{V} , the continuous sesquilinear form of \mathcal{B} defined in (2.3) is T -coercive on \tilde{V} such that

$$(4.2) \quad \varepsilon_0 \|v\|_a^2 \leq \mathcal{B}(v, \mathcal{T}_H v), \quad \forall v \in \tilde{V}.$$

where ε_0 is a positive constant depending on the high-contrast ratio Υ .

Proof. The technique that we utilize here is introducing a modified \mathcal{T} operator, denoted as \mathcal{T}_H , defined on \tilde{V} and $\mathcal{Q}_H : L^2 \rightarrow V$ is the operator from Lemma 4.6, then we have \mathcal{T}_H defined as follows:

$$\begin{aligned} \mathcal{T}_H v &= \mathcal{T}v - \mathcal{Q}_H \pi \mathcal{T}v = \begin{cases} v_1 - \mathcal{Q}_H \pi v_1, & \text{in } \Omega^+, \\ -v_2 + 2\mathcal{R}v_1 + \mathcal{Q}_H \pi v_2 - 2\mathcal{Q}_H \pi \mathcal{R}v_1, & \text{in } \Omega^-. \end{cases} \\ &= \begin{cases} v_1, & \text{in } \Omega^+, \\ -v_2 + 2(\mathcal{R} - \mathcal{Q}_H \pi \mathcal{R})v_1 = -v_2 + 2\mathcal{R}'_H v_1, & \text{in } \Omega^-. \end{cases} \end{aligned}$$

Here, the terms $\mathcal{Q}_H \pi v_1$ and $\mathcal{Q}_H \pi v_2$ vanish because $\pi v = 0$ on each coarse element, and meanwhile $\mathcal{Q}_H \pi v|_{K_i}$ depends only on $\pi v|_{K_i}$. Recalling the boundness of \mathcal{Q}_H , we can see that \mathcal{T}_H is a bounded operator that maps from \tilde{V} to \tilde{V} . Then, let

$$\mathcal{B}(v, \mathcal{T}_H v) = \underbrace{a(v, \mathcal{T}_H v)}_{I_1} - \underbrace{k^2 (cv, \mathcal{T}_H v)}_{I_2}.$$

For I_1 , we already know that from [27],

$$I_1 = a(v, \mathcal{T}_H v) \geq (1 - \sqrt{\Upsilon^{-1}} \|\mathcal{R}'_H\|_1) \|v\|_{\bar{a}}^2,$$

where $\|\mathcal{R}'_H\|_1$ should be understood as a positive constant such that for all $v \in \Omega^+$. For I_2 , by using of the resolution condition, we have

$$\begin{aligned} |I_2| &\leq k^2 \mu_{\text{msh}}^{-1} H^2 \int_{\Omega} |c| \mu_{\text{msh}} H^{-2} |v| |\mathcal{T}_H v| \, dx \leq C_1 k^2 \mu_{\text{msh}}^{-1} H^2 \|v\|_s^2 \\ &\leq C_1 k^2 \mu_{\text{msh}}^{-1} H^2 \left(\frac{1}{\Lambda} \|v\|_{\bar{a}}^2 + \|\pi v\|_s^2 \right) = C_1 k^2 \mu_{\text{msh}}^{-1} H^2 \Lambda^{-1} \|v\|_{\bar{a}}^2. \end{aligned}$$

We finally obtain

$$\begin{aligned} \mathcal{B}(v, \mathcal{T}_H v) &\geq \left(1 - \sqrt{\Upsilon^{-1}} \|\mathcal{R}'_H\|_1 - C_1 k^2 \mu_{\text{msh}}^{-1} H^2 \Lambda^{-1} \right) \|v\|_{\bar{a}}^2 \\ &\geq \left(1 - \sqrt{\Upsilon^{-1}} \|\mathcal{R}'_H\|_1 - C_* \right) \|v\|_{\bar{a}}^2 \\ &\geq \varepsilon_0 \|v\|_{\bar{a}}^2. \end{aligned}$$

where ε_0 is a positive constant depending on Υ . When we choose Υ to be a large value, the resolution condition (4.1) can guarantee ε_0 to be always positive. \square

We define the global operator $\mathcal{G}_i^\infty: L^2(\Omega) \rightarrow V = H_0^1(\Omega)$ corresponding to the coarse element K_i via the following variational problem:

$$(4.3) \quad \text{find } \mathcal{G}_i^\infty \psi \in V \text{ s.t. } \forall w \in V, \mathcal{B}(\mathcal{G}_i^\infty \psi, w) + s(\pi \mathcal{G}_i^\infty \psi, \pi w) = s(\pi \psi, \pi w)_{K_i}.$$

We reiterate several important facts here: the bilinear form is $s(\cdot, \cdot)$ defined on $L^2(\Omega) \times L^2(\Omega)$ as

$$s(v, w) = \int_{\Omega} \mu v w \, dx = \mu_{\text{msh}} \sum_{i=1}^N \text{diam}(K_i)^{-2} \int_{K_i} c v w \, dx.$$

The global solution is defined by solving the following variational form:

$$(4.4) \quad \text{find } u_{\text{glo}} \in V_{\text{glo}}, \text{ s.t. } \forall v \in V_{\text{glo}}, \mathcal{B}(u_{\text{glo}}, v) = (f, v).$$

To guarantee the well-posedness of (4.4), we need to examine the inf-sup stability of V_{glo} , i.e., proving the existence of a uniform lower bound of

$$(4.5) \quad \inf_{u_{\text{glo}} \in V_{\text{glo}}} \sup_{w_{\text{glo}} \in V_{\text{glo}}} \frac{\mathcal{B}(u_{\text{glo}}, w_{\text{glo}})}{\|u_{\text{glo}}\|_{\bar{a}} \|w_{\text{glo}}\|_{\bar{a}}}.$$

The Fortin trick suggests that it suffices to check that

$$\inf_{u \in \tilde{V}} \sup_{w \in \tilde{V}} \frac{\mathcal{B}(u, w)}{\|u\|_{\bar{a}} \|w\|_{\bar{a}}} \geq \beta_{\text{glo}}$$

holds. Then, we reduce the proof of the inf-sup stability of $\mathcal{B}(v, \mathcal{T}_H v)$ for all $v \in \tilde{V}$.

THEOREM 4.2. *Let u be the solution to the original problem (2.4) and u_{glo} be the solution to the global problem (4.4). If $f \in L^2(\Omega)$, then*

$$\|u - u_{\text{glo}}\|_{\bar{a}} \leq \frac{\|f\|_{s^{-1}}}{\sqrt{\Lambda}}.$$

Proof. For the global error estimate in the energy norm, we can obtain

$$\begin{aligned} \|u - u_{\text{glo}}\|_{\bar{a}}^2 &\leq \frac{1}{\varepsilon_0} \mathcal{B}(u - u_{\text{glo}}, \mathcal{T}_H(u - u_{\text{glo}})) = \frac{1}{\varepsilon_0} \mathcal{B}(u, \mathcal{T}_H(u - u_{\text{glo}})) \\ &= (f, \mathcal{T}_H(u - u_{\text{glo}})) \leq C_1 \|f\|_{\bar{s}-1} \|u - u_{\text{glo}}\|_{\bar{s}} \leq \frac{C_1 \|f\|_{\bar{s}-1}}{\sqrt{\Lambda}} \|u - u_{\text{glo}}\|_{\bar{a}}, \end{aligned}$$

where the last inequality comes from the fact that $\mathcal{T}_H(u - u_{\text{glo}}) \in \tilde{V}$ for $u - u_{\text{glo}} \in \tilde{V}$ and the use of the [Lemma 3.1](#), the last second inequality comes from the boundedness of the \mathcal{T}_H under the s -norm, where

$$\|f\|_{\bar{s}-1} := \left(\int_{\Omega} |\mu|^{-1} |f|^2 dx \right)^{1/2} \approx \mathcal{O}(H). \quad \square$$

Due to the incompatibility between the definition of an oversampling region K_i^m and T-coercivity, we need to introduce the method called symmetrization [8] to construct new subdomains so that we can prove the exponential decay of multiscale basis functions outside those symmetric patches in [Lemma 4.3](#). We add a hat notation “ $\hat{\cdot}$ ” (e.g., $\hat{V}_i^m = H_0^1(\hat{K}_i^m)$) to indicate that this term is associated with \hat{K}_i^m rather than K_i^m . Similarly, we can obtain the well-posedness of the modified local operator $\hat{\mathcal{G}}_i^m$ associated with the coarse element K_i :

$$(4.6) \quad \begin{aligned} &\text{find } \hat{\mathcal{G}}_i^m \psi \in \hat{V}_i^m \text{ s.t. } \forall v \in \hat{V}_i^m, \\ &\mathcal{B}(\hat{\mathcal{G}}_i^m \psi, w)_{\hat{K}_i^m} + s(\pi \hat{\mathcal{G}}_i^m \psi, \pi w)_{\hat{K}_i^m} = s(\pi \psi, \pi w)_{K_i}. \end{aligned}$$

ASSUMPTION I. *There exists a list of subdomains $\{\hat{K}_i^1, \hat{K}_i^2, \dots\}$ that fulfills the requirements listed below:*

1. *Each \hat{K}_i^m consists of coarse elements from \mathcal{K}_H .*
2. *There exists an inclusion relation $K_i \subset \hat{K}_i^1 \subset \hat{K}_i^2 \subset \dots \subset$, such that $\text{dist}(\partial \hat{K}_i^m, \partial \hat{K}_i^{m+1}) \geq C_{\text{msh}} H$.*
3. *For any $v \in V$ with $\text{supp } v \subset \overline{\hat{K}_i^m}$ or $\overline{\Omega \setminus \hat{K}_i^m}$, it holds that $\text{supp } \mathcal{T}v \subset \overline{\hat{K}_i^m}$ or $\overline{\Omega \setminus \hat{K}_i^m}$ accordingly.*

Before we provide the detailed proof of [Lemma 4.3](#), we need to define the cutoff functions with respect to these oversampling domains as follows. We define a cut-off function $\hat{\eta}_i^{m-1, m} \in C^{0,1}(\Omega)$ as

$$\hat{\eta}_i^{m-1, m} = \begin{cases} 1, & \text{in } \hat{K}_i^{m-1}, \\ 0, & \text{in } \Omega \setminus \hat{K}_i^m, \end{cases}$$

with $0 \leq \hat{\eta}_i^{m-1, m} \leq 1$ in $\hat{K}_i^m \setminus \hat{K}_i^{m-1}$. By using controlling the parameter μ_{msh} , we can derive the inequality

$$\left| \nabla \hat{\eta}_i^{m-1, m} \right|^2 |\sigma| \leq |\mu|$$

on Ω for i and m .

ASSUMPTION II. *The number of coarse elements within \hat{K}_i^m satisfies a relation:*

$$\#\{K \in \mathcal{K}_H \mid K \subset \hat{K}_i^m\} \leq C_{\text{ol}} m^d,$$

where C_{ol} depends solely on the mesh quality.

LEMMA 4.3. *There exists a positive constant θ with $\theta < 1$ that independents on k, m and H such that for any $m \geq 1, 1 \leq i \leq N_{elem}$ and $\psi \in L^2(\Omega)$,*

$$\|\mathcal{G}_i^\infty \psi\|_{\bar{a}, \Omega \setminus \hat{K}_i^m}^2 + \|\pi \mathcal{G}_i^\infty \psi\|_{\bar{s}, \Omega \setminus \hat{K}_i^m}^2 \leq \theta^m (\|\mathcal{G}_i^\infty \psi\|_{\bar{a}}^2 + \|\pi \mathcal{G}_i^\infty \psi\|_{\bar{s}}^2),$$

where $\theta = \left(1 + \left(\frac{C}{2C_0 + C_1 + C_* \Lambda}\right)^2\right)^{-1} < 1$.

Proof. Taking $z_i = (1 - \hat{\eta}_i^{m-1, m}) \mathcal{G}_i^\infty \psi$, we can see that z_i is supported in $\Omega \setminus \hat{K}_i^{m-1}$. Substituting $\mathcal{T} z_i$ for w in the variational form (4.3), we have

$$\mathcal{B}(\mathcal{G}_i^\infty \psi, \mathcal{T} z_i) + s(\pi \mathcal{G}_i^\infty \psi, \pi \mathcal{T} z_i) = 0.$$

As a result, we can formulate a decomposition as follows:

$$\begin{aligned} a(z_i, \mathcal{T} z_i) + s(\pi z_i, \pi \mathcal{T} z_i) &= -a(\hat{\eta}_i^{m-1, m} \mathcal{G}_i^\infty \psi, \mathcal{T} z_i) - s(\pi(\hat{\eta}_i^{m-1, m} \mathcal{G}_i^\infty \psi), \pi \mathcal{T} z_i) + k^2 (c \mathcal{G}_i^\infty \psi, \mathcal{T} z_i) \\ &= - \underbrace{\int_{\Omega} \sigma \mathcal{G}_i^\infty \psi \nabla \hat{\eta}_i^{m-1, m} \cdot \nabla \mathcal{T} z_i \, dx}_{I_1} - \underbrace{\int_{\Omega} \sigma \hat{\eta}_i^{m-1, m} \nabla \mathcal{G}_i^\infty \psi \cdot \nabla \mathcal{T} z_i \, dx}_{I_2} \\ &\quad - \underbrace{\int_{\Omega} \mu \pi(\hat{\eta}_i^{m-1, m} \mathcal{G}_i^\infty \psi) \cdot \pi \mathcal{T} z_i \, dx}_{I_3} + \underbrace{k^2 \int_{\Omega} c \mathcal{G}_i^\infty \psi \cdot \mathcal{T} z_i \, dx}_{I_4} \end{aligned}$$

For I_1 , by the Cauchy-Schwarz inequality, it is evident that

$$\begin{aligned} |I_1| &\leq \left(\int_{\Omega} |\sigma| \left| \nabla \hat{\eta}_i^{m-1, m} \right|^2 |\mathcal{G}_i^\infty \psi|^2 \, dx \right)^{1/2} \left(\int_{\Omega} |\sigma| |\nabla \mathcal{T} z_i|^2 \, dx \right)^{1/2} \\ &\leq \|\mathcal{G}_i^\infty \psi\|_{\bar{s}, \hat{K}_i^m \setminus \hat{K}_i^{m-1}} \|\mathcal{T} z_i\|_{\bar{a}, \Omega \setminus \hat{K}_i^{m-1}} \\ &\leq C_0 \left(\|\pi \mathcal{G}_i^\infty \psi\|_{\bar{s}, \hat{K}_i^m \setminus \hat{K}_i^{m-1}}^2 + \Lambda^{-1} \|\mathcal{G}_i^\infty \psi\|_{\bar{a}, \hat{K}_i^m \setminus \hat{K}_i^{m-1}}^2 \right)^{1/2} \|z_i\|_{\bar{a}, \Omega \setminus \hat{K}_i^{m-1}}, \end{aligned}$$

where the last line follows from (3.7) and (3.3). For I_2 , we have

$$\begin{aligned} |I_2| &\leq \left(\int_{\hat{K}_i^m \setminus \hat{K}_i^{m-1}} |\sigma| \left| \hat{\eta}_i^{m-1, m} \right|^2 |\nabla \mathcal{G}_i^\infty \psi|^2 \, dx \right)^{1/2} \left(\int_{\Omega} |\sigma| |\nabla \mathcal{T} z_i|^2 \, dx \right)^{1/2} \\ &\leq \|\mathcal{G}_i^\infty \psi\|_{\bar{a}, \hat{K}_i^m \setminus \hat{K}_i^{m-1}} \|\mathcal{T} z_i\|_{\bar{a}, \Omega \setminus \hat{K}_i^{m-1}} \leq C_0 \|\mathcal{G}_i^\infty \psi\|_{\bar{a}, \hat{K}_i^m \setminus \hat{K}_i^{m-1}} \|z_i\|_{\bar{a}, \Omega \setminus \hat{K}_i^{m-1}}. \end{aligned}$$

For I_3 , we can similarly show that

$$\begin{aligned} |I_3| &\leq \left(\int_{\hat{K}_i^m \setminus \hat{K}_i^{m-1}} |\mu| \left| \pi(\hat{\eta}_i^{m-1, m} \mathcal{G}_i^\infty \psi) \right|^2 \, dx \right)^{1/2} \left(\int_{\Omega} |\mu| |\pi \mathcal{T} z_i|^2 \, dx \right)^{1/2} \\ &= \|\pi(\hat{\eta}_i^{m-1, m} \mathcal{G}_i^\infty \psi)\|_{\bar{s}, \hat{K}_i^m \setminus \hat{K}_i^{m-1}} \|\pi \mathcal{T} z_i\|_{\bar{s}, \Omega \setminus \hat{K}_i^{m-1}} \\ &\leq \|\hat{\eta}_i^{m-1, m} \mathcal{G}_i^\infty \psi\|_{\bar{s}, \hat{K}_i^m \setminus \hat{K}_i^{m-1}} \|\mathcal{T} z_i\|_{\bar{s}, \Omega \setminus \hat{K}_i^{m-1}} \\ &\leq C_1 \|\mathcal{G}_i^\infty \psi\|_{\bar{s}, \hat{K}_i^m \setminus \hat{K}_i^{m-1}} \|z_i\|_{\bar{s}, \Omega \setminus \hat{K}_i^{m-1}} \\ &\leq C_1 \left(\|\pi \mathcal{G}_i^\infty \psi\|_{\bar{s}, \hat{K}_i^m \setminus \hat{K}_i^{m-1}}^2 + \Lambda^{-1} \|\mathcal{G}_i^\infty \psi\|_{\bar{a}, \hat{K}_i^m \setminus \hat{K}_i^{m-1}}^2 \right)^{1/2} \left(\|\pi z_i\|_{\bar{s}, \Omega \setminus \hat{K}_i^{m-1}}^2 + \Lambda^{-1} \|z_i\|_{\bar{a}, \Omega \setminus \hat{K}_i^{m-1}}^2 \right)^{1/2}. \end{aligned}$$

For I_4 , by using of the resolution condition (4.1) and (3.8), we have

$$\begin{aligned}
|I_4| &\leq k^2 \mu_{\text{msh}}^{-1} H^2 \int_{\Omega} |c \mu_{\text{msh}} H^{-2} |z_i + \hat{\eta}_i^{m-1, m} \hat{\mathcal{G}}_i^\infty \psi| \cdot |\mathcal{T} z_i| dx \\
&\leq k^2 \mu_{\text{msh}}^{-1} H^2 \|z_i\|_{\bar{s}, \Omega \setminus \hat{K}_i^{m-1}} \|\mathcal{T} z_i\|_{\bar{s}, \Omega \setminus \hat{K}_i^{m-1}} + k^2 \mu_{\text{msh}}^{-1} H^2 \|\mathcal{G}_i^\infty \psi\|_{\bar{s}, \hat{K}_i^m \setminus \hat{K}_i^{m-1}} \|\mathcal{T} z_i\|_{\bar{s}, \Omega \setminus \hat{K}_i^{m-1}} \\
&\leq C_1 k^2 \mu_{\text{msh}}^{-1} H^2 \|z_i\|_{\bar{s}, \Omega \setminus \hat{K}_i^{m-1}}^2 + C_1 k^2 \mu_{\text{msh}}^{-1} H^2 \|\mathcal{G}_i^\infty \psi\|_{\bar{s}, \hat{K}_i^m \setminus \hat{K}_i^{m-1}} \|z_i\|_{\bar{s}, \Omega \setminus \hat{K}_i^{m-1}} \\
&\leq C_* \Lambda \left(\Lambda^{-1} \|z_i\|_{\bar{a}, \Omega \setminus \hat{K}_i^{m-1}}^2 + \|\pi z_i\|_{\bar{s}, \Omega \setminus \hat{K}_i^{m-1}}^2 \right) \\
&\quad + C_* \Lambda \left(\Lambda^{-1} \|\hat{\mathcal{G}}_i^\infty \psi\|_{\bar{a}, \hat{K}_i^m \setminus \hat{K}_i^{m-1}}^2 + \|\pi \hat{\mathcal{G}}_i^\infty \psi\|_{\bar{s}, \hat{K}_i^m \setminus \hat{K}_i^{m-1}}^2 \right)^{1/2} \|z_i\|_{\bar{s}, \Omega \setminus \hat{K}_i^{m-1}}.
\end{aligned}$$

Recalling (3.5) and (3.6), providing that $\frac{1}{\Lambda}$ and C_* are small enough ($\frac{1}{\Lambda}, C_* \leq 1$), we can obtain that

$$\begin{aligned}
a(z_i, \mathcal{T} z_i) + s(\pi z_i, \pi \mathcal{T} z_i) &\geq \left(\underbrace{(C_2 - C_*)}_{p_1} \|z_i\|_{\bar{a}, \Omega \setminus \hat{K}_i^{m-1}}^2 + \underbrace{(C_2 - C_* \Lambda)}_{p_2} \|\pi z_i\|_{\bar{s}, \Omega \setminus \hat{K}_i^{m-1}}^2 \right) \\
&\geq C \left(\|z_i\|_{\bar{a}, \Omega \setminus \hat{K}_i^{m-1}}^2 + \|\pi z_i\|_{\bar{s}, \Omega \setminus \hat{K}_i^{m-1}}^2 \right),
\end{aligned}$$

where $p_1 \geq p_2 \geq 0$, for simplicity, we denote $C = \min\{C_2 - C_*, C_2 - C_* \Lambda\}$. Due to $\frac{1}{\Lambda}$ is small enough ($\frac{1}{\Lambda} \leq 1$), we have

$$\begin{aligned}
&\left(\|\mathcal{G}_i^\infty \psi\|_{\bar{a}, \Omega \setminus \hat{K}_i^m}^2 + \|\pi \mathcal{G}_i^\infty \psi\|_{\bar{s}, \Omega \setminus \hat{K}_i^m}^2 \right)^{1/2} \leq \left(\|z_i\|_{\bar{a}, \Omega \setminus \hat{K}_i^{m-1}}^2 + \|\pi z_i\|_{\bar{s}, \Omega \setminus \hat{K}_i^{m-1}}^2 \right)^{1/2} \\
&\leq \frac{2C_0 + C_1 + C_* \Lambda}{C} \left(\|\mathcal{G}_i^\infty \psi\|_{\bar{a}, \hat{K}_i^m \setminus \hat{K}_i^{m-1}}^2 + \|\pi \mathcal{G}_i^\infty \psi\|_{\bar{s}, \hat{K}_i^m \setminus \hat{K}_i^{m-1}}^2 \right)^{1/2}.
\end{aligned}$$

We hence derive an iteration relation

$$\begin{aligned}
&\|\mathcal{G}_i^\infty \psi\|_{\bar{a}, \Omega \setminus \hat{K}_i^m}^2 + \|\pi \mathcal{G}_i^\infty \psi\|_{\bar{s}, \Omega \setminus \hat{K}_i^m}^2 \\
&\leq \left(1 + \left(\frac{C}{2C_0 + C_1 + C_* \Lambda} \right)^2 \right)^{-1} \left(\|\mathcal{G}_i^\infty \psi\|_{\bar{a}, \Omega \setminus \hat{K}_i^{m-1}}^2 + \|\pi \mathcal{G}_i^\infty \psi\|_{\bar{s}, \Omega \setminus \hat{K}_i^{m-1}}^2 \right),
\end{aligned}$$

which completes the proof. \square

LEMMA 4.4. *It holds that for any $m \geq 1, 1 \leq i \leq N$ and $\psi \in L^2(\Omega)$,*

$$\|(\mathcal{G}_i^\infty - \hat{\mathcal{G}}_i^m) \psi\|_{\bar{a}}^2 + \|\pi(\mathcal{G}_i^\infty - \hat{\mathcal{G}}_i^m) \psi\|_{\bar{s}}^2 \leq C' \theta^{m-1} \left(\|\mathcal{G}_i^\infty \psi\|_{\bar{a}}^2 + \|\pi \mathcal{G}_i^\infty \psi\|_{\bar{s}}^2 \right),$$

where $\theta < 1$ comes from Lemma 4.3 and $C' = \left(\frac{4C_0 + C_1 + C_* \Lambda}{C} \right)^2 > 0$ depends on C, C_0, C_1, C_* and Λ .

Proof. We now take $z_i = (\mathcal{G}_i^\infty - \hat{\mathcal{G}}_i^m) \psi$ and introduce a decomposition

$$z_i = \underbrace{(1 - \hat{\eta}_i^{m-1, m}) \mathcal{G}_i^\infty \psi}_{z_i'} + \underbrace{(\hat{\eta}_i^{m-1, m} - 1) \hat{\mathcal{G}}_i^m \psi + \hat{\eta}_i^{m-1, m} z_i}_{z_i''}.$$

We can observe that $z_i'' \in \hat{V}_i^m$, which implies $\mathcal{T} z_i'' \in \hat{V}_i^m$. Therefore, it is easy to see that $\mathcal{B}(z_i, \mathcal{T} z_i'') + s(\pi z_i, \pi \mathcal{T} z_i'') = 0$. Now we start to estimate $\mathcal{B}(z_i, \mathcal{T} z_i') + s(\pi z_i, \pi \mathcal{T} z_i')$, and the next step is

$$a(z_i, \mathcal{T} z_i) + s(\pi z_i, \mathcal{T} z_i) = \mathcal{B}(z_i, \mathcal{T} z_i) + s(\pi z_i, \mathcal{T} z_i) + k^2(z_i, \mathcal{T} z_i)$$

$$\begin{aligned}
&= \mathcal{B}(z_i, \mathcal{T}z'_i) + s(\pi z_i, \pi \mathcal{T}z'_i) + k^2(z_i, \mathcal{T}z_i) \\
&= a(z_i, \mathcal{T}z'_i) + s(\pi z_i, \pi \mathcal{T}z'_i) + k^2(z_i, \mathcal{T}z''_i) \\
&\leq \underbrace{\|z_i\|_{\bar{a}} \|\mathcal{T}z'_i\|_{\bar{a}}}_{I_1} + \underbrace{k^2(z_i, \mathcal{T}z''_i)}_{I_2} + \underbrace{\|\pi z_i\|_{\bar{s}} \|\pi \mathcal{T}z'_i\|_{\bar{s}}}_{I_3}.
\end{aligned}$$

For I_1 , we recall that $\|\mathcal{T}z'_i\|_{\bar{a}} \leq C_0 \|z'_i\|_{\bar{a}}$, and for z'_i we have

$$\begin{aligned}
\|z'_i\|_{\bar{a}}^2 &\leq 2 \int_{\Omega \setminus \hat{K}_i^{m-1}} |\sigma| \left| 1 - \hat{\eta}_i^{m-1, m} \right|^2 \left| \nabla \hat{\mathcal{G}}_i^\infty \psi \right|^2 dx + 2 \int_{\hat{K}_i^m \setminus \hat{K}_i^{m-1}} |\sigma| \left| \nabla \hat{\eta}_i^{m-1, m} \right|^2 \left| \hat{\mathcal{G}}_i^\infty \psi \right|^2 dx \\
&\leq 2 \|\mathcal{G}_i^\infty \psi\|_{\bar{a}, \Omega \setminus \hat{K}_i^{m-1}}^2 + 2 \int_{\Omega \setminus \hat{K}_i^{m-1}} |\mu| |\mathcal{G}_i^\infty \psi|^2 dx \\
&\leq 2(1 + \Lambda^{-1}) \|\mathcal{G}_i^\infty \psi\|_{\bar{a}, \Omega \setminus \hat{K}_i^{m-1}}^2 + 4 \|\pi \mathcal{G}_i^\infty \psi\|_{\bar{s}, \Omega \setminus \hat{K}_i^{m-1}}^2. \quad \blacksquare
\end{aligned}$$

For I_2 , we use the resolution condition (4.1) and the definition of z''_i to obtain

$$\begin{aligned}
|I_2| &\leq k^2 \mu_{\text{msh}}^{-1} H^2 \int_{\Omega} |c| \mu_{\text{msh}} H^{-2} |z_i| \cdot |\mathcal{T}z''_i| dx \leq C_1 k^2 \mu_{\text{msh}}^{-1} H^2 \|z_i\|_{\bar{s}} \|z''_i\|_{\bar{s}} \\
&\leq C_* \Lambda (\|z_i\|_{\bar{s}}^2 + \|z_i\|_{\bar{s}} \|z'_i\|_{\bar{s}}) \\
&\leq C_* \Lambda (\Lambda^{-1} \|z_i\|_{\bar{a}}^2 + \|\pi z_i\|_{\bar{s}}^2) + C_* \Lambda (\Lambda^{-1} \|z_i\|_{\bar{a}}^2 + \|\pi z_i\|_{\bar{s}}^2)^{1/2} \|z'_i\|_{\bar{s}}.
\end{aligned}$$

For I_3 , $\|\pi \mathcal{T}z'_i\|_{\bar{s}} \leq \|\mathcal{T}z'_i\|_{\bar{s}} \leq C_1 \|z'_i\|_{\bar{s}}$ and

$$\begin{aligned}
\|z'_i\|_{\bar{s}}^2 &= \int_{\Omega} |\mu| \left| 1 - \hat{\eta}_i^{m-1, m} \right|^2 |\mathcal{G}_i^\infty \psi|^2 dx \leq \|\mathcal{G}_i^\infty \psi\|_{\bar{s}, \Omega \setminus \hat{K}_i^{m-1}}^2 \\
&\leq \Lambda^{-1} \|\mathcal{G}_i^\infty \psi\|_{\bar{a}, \Omega \setminus \hat{K}_i^{m-1}}^2 + \|\pi \mathcal{G}_i^\infty \psi\|_{\bar{s}, \Omega \setminus \hat{K}_i^{m-1}}^2.
\end{aligned}$$

Then, providing that $\frac{1}{\Lambda}$ and C_* is small enough ($\frac{1}{\Lambda}, C_* \leq 1$), we have the following estimate

$$C \left(\|z_i\|_{\bar{a}}^2 + \|\pi z_i\|_{\bar{s}}^2 \right) \leq a(z_i, \mathcal{T}z_i) + s(\pi z_i, \pi \mathcal{T}z_i),$$

We finally have can obtain that

$$\|z_i\|_{\bar{a}}^2 + \|\pi z_i\|_{\bar{s}}^2 \leq \left(\frac{4C_0 + C_1 + C_* \Lambda}{C} \right)^2 \left(\|\mathcal{G}_i^\infty \psi\|_{\bar{a}, \Omega \setminus \hat{K}_i^{m-1}}^2 + \|\pi \mathcal{G}_i^\infty \psi\|_{\bar{s}, \Omega \setminus \hat{K}_i^{m-1}}^2 \right),$$

And we hence derive the desired result by utilizing Lemma 4.3. \square

THEOREM 4.5. *Under assumption II, there exists constants Υ, Λ^* such that for any $\Upsilon \geq \Upsilon'$ and $\Lambda \geq \Lambda^*$, it holds that for any $m \geq 1, 1 \leq i \leq N$ and any $\psi \in L^2(\Omega)$,*

$$\|(\mathcal{G}^\infty - \hat{\mathcal{G}}^m)\psi\|_{\bar{a}}^2 + \|\pi(\mathcal{G}^\infty - \hat{\mathcal{G}}^m)\psi\|_{\bar{s}}^2 \leq c_0(\Lambda) C_{\text{ol}}(m+1)^d \theta^{m-1} \|\pi\psi\|_{\bar{s}}^2,$$

where $\theta < 1$ from Lemma 4.3 and $c_0(\Lambda) > 0$ depends on $\Lambda, C, C_*, C_0, C_1$, and C_2 .

Proof. We denote $z_i = (\mathcal{G}_i^\infty - \hat{\mathcal{G}}_i^m)\psi$ and $z = \sum_{i=1}^N z_i$. Then we take the decomposition of z as

$$z = \underbrace{(1 - \hat{\eta}_i^{m, m+1})z}_{z'} + \underbrace{\hat{\eta}_i^{m, m+1}z}_{z''}$$

where i is arbitrary chosen from $1, \dots, N$. We can observe that $\text{supp}(\mathcal{T}z') \cap K_i = \emptyset$, then we have $\mathcal{B}(z_i, \mathcal{T}z') + s(\pi z_i, \pi \mathcal{T}z') = 0$. The next step

$$\begin{aligned} a(z_i, \mathcal{T}z) + s(\pi z_i, \pi \mathcal{T}z) &= \mathcal{B}(z_i, \mathcal{T}z'') + s(\pi z_i, \pi \mathcal{T}z'') + k^2(z_i, \mathcal{T}z) \\ &= a(z_i, \mathcal{T}z'') + s(\pi z_i, \pi \mathcal{T}z'') + k^2(z_i, \mathcal{T}z') \\ &\leq \underbrace{\|z_i\|_{\bar{a}} \|\mathcal{T}z''\|_{\bar{a}}}_{I_1} + \underbrace{k^2(z_i, \mathcal{T}z')}_{I_2} + \underbrace{\|\pi z_i\|_{\bar{s}} \|\pi \mathcal{T}z''\|_{\bar{s}}}_{I_3}. \end{aligned}$$

Similarly, for $\|\mathcal{T}z''\|_{\bar{a}}$ in I_1 , by using (3.5)

$$\|\mathcal{T}z''\|_{\bar{a}} \leq C_0 \|\hat{\eta}_i^{m, m+1} z\|_{\bar{a}} \leq C_0 \left(\|z\|_{\bar{a}, \hat{K}_i^{m+1}} + \|z\|_{\bar{s}, \hat{K}_i^{m+1}} \right) \leq C_0 \left(\left(1 + \frac{1}{\sqrt{\Lambda}}\right) \|z\|_{\bar{a}, \hat{K}_i^{m+1}} + \|\pi z\|_{\bar{s}, \hat{K}_i^{m+1}} \right). \blacksquare$$

For $\|\pi \mathcal{T}z''\|_{\bar{s}}$ in I_3 , by using (3.8)

$$\|\pi \mathcal{T}z''\|_{\bar{s}} \leq \|\mathcal{T}z''\|_{\bar{s}} \leq C_1 \|\hat{\eta}_i^{m, m+1} z\|_{\bar{s}} \leq C_1 \|z\|_{\bar{s}, \hat{K}_i^{m+1}} \leq C_1 \left(\frac{1}{\sqrt{\Lambda}} \|z\|_{\bar{a}, \hat{K}_i^{m+1}} + \|\pi z\|_{\bar{s}, \hat{K}_i^{m+1}} \right) \blacksquare$$

For I_2 , we use the resolution condition (4.1) and inequality (3.8),

$$\begin{aligned} |I_2| &\leq k^2 \mu_{\text{msh}}^{-1} H^2 \int_{\Omega} |c| \mu_{\text{msh}} H^{-2} |z_i| \cdot |\mathcal{T}z'| \, dx \leq C_1 k^2 \mu_{\text{msh}}^{-1} H^2 \|z_i\|_{\bar{s}} \|z'\|_{\bar{s}} \\ &\leq C_* \Lambda \left(\|z\|_{\bar{s}}^2 + \|z_i\|_{\bar{s}} \|z\|_{\bar{s}, \hat{K}_i^{m+1}} \right) \\ &\leq C_* \Lambda \left(\Lambda^{-1} \|z\|_{\bar{a}}^2 + \|\pi z\|_{\bar{s}}^2 + \|z_i\|_{\bar{s}} \|z\|_{\bar{s}, \hat{K}_i^{m+1}} \right) \end{aligned}$$

To simplify the expression, we assume that $\frac{1}{\Lambda} \leq 1$, and combine the estimates of I_1, I_2 and I_3 to derive that

$$\begin{aligned} a(z_i, \mathcal{T}z) + s(\pi z_i, \pi \mathcal{T}z) &\leq \underbrace{(2C_0 + C_1 + C_* \Lambda)}_{c_0(\Lambda)} \left(\|z\|_{\bar{a}, \hat{K}_i^{m+1}}^2 + \|\pi z\|_{\bar{s}, \hat{K}_i^{m+1}}^2 \right)^{1/2} \left(\|z_i\|_{\bar{a}}^2 + \|\pi z_i\|_{\bar{s}}^2 \right)^{1/2} \\ &\quad + C_* \|z\|_{\bar{a}}^2 + C_* \Lambda \|\pi z\|_{\bar{s}}^2, \end{aligned} \blacksquare$$

where $c_0(\Lambda)$ depends on Λ, C_0, C_1 , and C_2 . Based on the oversampling condition [assumption II](#), it holds that

$$\sum_{i=1}^{N_{\text{elem}}} \left(\|z\|_{\bar{a}, \hat{K}_i^{m+1}}^2 + \|\pi z\|_{\bar{s}, \hat{K}_i^{m+1}}^2 \right) \leq C_{\text{ol}} (m+1)^d \left(\|z\|_{\bar{a}}^2 + \|\pi z\|_{\bar{s}}^2 \right).$$

Therefore, applying the Cauchy–Schwarz inequality,

$$\begin{aligned} C'' \left(\|z\|_{\bar{a}}^2 + \|\pi z\|_{\bar{s}}^2 \right) &\leq \sum_{i=1}^{N_{\text{elem}}} (a(z_i, \mathcal{T}z) + s(\pi z_i, \pi \mathcal{T}z)) \\ &\leq c_0(\Lambda) \left(\sum_{i=1}^{N_{\text{elem}}} \left(\|z\|_{\bar{a}, \hat{K}_i^{m+1}}^2 + \|\pi z\|_{\bar{s}, \hat{K}_i^{m+1}}^2 \right) \right)^{1/2} \left(\sum_{i=1}^{N_{\text{elem}}} \left(\|z_i\|_{\bar{a}}^2 + \|\pi z_i\|_{\bar{s}}^2 \right) \right)^{1/2} \\ &\leq c_0(\Lambda) \sqrt{C_{\text{ol}}} (m+1)^{d/2} \left(\|z\|_{\bar{a}}^2 + \|\pi z\|_{\bar{s}}^2 \right)^{1/2} \left(\sum_{i=1}^{N_{\text{elem}}} \left(\|z_i\|_{\bar{a}}^2 + \|\pi z_i\|_{\bar{s}}^2 \right) \right)^{1/2}, \end{aligned}$$

where $C''' = \max\{C_2 - C_*N, C_2 - C_*\Lambda N\} > 0$. It has been shown in [Lemma 4.4](#) that, for any i ,

$$\|z_i\|_{\bar{a}}^2 + \|\pi z_i\|_{\bar{s}}^2 \leq C'\theta^{m-1} \left(\|\mathcal{G}_i^\infty \psi\|_{\bar{a}}^2 + \|\pi \mathcal{G}_i^\infty \psi\|_{\bar{s}}^2 \right),$$

and we turn to provide a bound on $\sum_{i=1}^{N_{\text{elem}}} \|\mathcal{G}_i^\infty \psi\|_{\bar{a}}^2 + \|\pi \mathcal{G}_i^\infty \psi\|_{\bar{s}}^2$ by letting $w = \mathcal{G}_i^\infty \psi$ in [\(4.3\)](#) to obtain

$$\begin{aligned} & C_2 \left(\|\mathcal{G}_i^\infty \psi\|_{\bar{a}}^2 + \|\pi \mathcal{G}_i^\infty \psi\|_{\bar{s}}^2 \right) \leq a(\mathcal{G}_i^\infty \psi, \mathcal{T} \mathcal{G}_i^\infty \psi) + s(\pi \mathcal{G}_i^\infty \psi, \pi \mathcal{T} \mathcal{G}_i^\infty \psi) \\ & = s(\pi \psi, \pi \mathcal{T} \mathcal{G}_i^\infty \psi)_{K_i} + k^2(\mathcal{G}_i^\infty \psi, \mathcal{T} \mathcal{G}_i^\infty \psi) \\ & \leq \|\pi \psi\|_{\bar{s}, K_i} \|\pi \mathcal{T} \mathcal{G}_i^\infty \psi\|_{\bar{s}, K_i} + \underbrace{k^2(\mathcal{G}_i^\infty \psi, \mathcal{T} \mathcal{G}_i^\infty \psi)}_{I_1} \\ & \leq \|\pi \psi\|_{\bar{s}, K_i} \|\mathcal{T} \mathcal{G}_i^\infty \psi\|_{\bar{s}} + C_* \Lambda (\Lambda^{-1} \|\mathcal{G}_i^\infty \psi\|_{\bar{a}}^2 + \|\pi \mathcal{G}_i^\infty \psi\|_{\bar{s}}^2) \\ & \leq C_1 \|\pi \psi\|_{\bar{s}, K_i} \|\mathcal{G}_i^\infty \psi\|_{\bar{s}} + C_* \Lambda (\Lambda^{-1} \|\mathcal{G}_i^\infty \psi\|_{\bar{a}}^2 + \|\pi \mathcal{G}_i^\infty \psi\|_{\bar{s}}^2) \\ & \leq C_1 \|\pi \psi\|_{\bar{s}, K_i} \left(\Lambda^{-1} \|\mathcal{G}_i^\infty \psi\|_{\bar{a}}^2 + \|\pi \mathcal{G}_i^\infty \psi\|_{\bar{s}}^2 \right)^{1/2} + C_* \Lambda (\Lambda^{-1} \|\mathcal{G}_i^\infty \psi\|_{\bar{a}}^2 + \|\pi \mathcal{G}_i^\infty \psi\|_{\bar{s}}^2), \end{aligned}$$

where for the boundedness of I_1 , we use the resolution condition [\(4.1\)](#) and [\(3.8\)](#)

$$\begin{aligned} |I_1| & \leq k^2 \mu_{\text{msh}}^{-1} H^2 \int_{\Omega} |c| \mu_{\text{msh}} H^{-2} |\mathcal{G}_i^\infty \psi| \cdot |\mathcal{T} \mathcal{G}_i^\infty \psi| \, dx \\ & \leq C_1 k^2 \mu_{\text{msh}}^{-1} H^2 \|\mathcal{G}_i^\infty \psi\|_{\bar{s}}^2 \leq C_* \Lambda (\Lambda^{-1} \|\mathcal{G}_i^\infty \psi\|_{\bar{a}}^2 + \|\pi \mathcal{G}_i^\infty \psi\|_{\bar{s}}^2). \end{aligned}$$

Finally, the above gives that

$$\begin{aligned} C(\|\mathcal{G}_i^\infty \psi\|_{\bar{a}}^2 + \|\pi \mathcal{G}_i^\infty \psi\|_{\bar{s}}^2) & \leq (C_2 - C_*) \|\mathcal{G}_i^\infty \psi\|_{\bar{a}}^2 + (C_2 - C_* \Lambda) \|\pi \mathcal{G}_i^\infty \psi\|_{\bar{s}}^2 \leq c_1 \|\pi \psi\|_{\bar{s}, K_i}^2 \\ \|\mathcal{G}_i^\infty \psi\|_{\bar{a}}^2 + \|\pi \mathcal{G}_i^\infty \psi\|_{\bar{s}}^2 & \leq c_1 \|\pi \psi\|_{\bar{s}, K_i}^2, \end{aligned}$$

where $c_1 = (C_1/C)^2 > 0$. We finally completed the proof by collecting all the estimates obtained above. \square

LEMMA 4.6 (ref. [\[11\]](#)). *There exists a bounded map $\mathcal{Q}_H: L^2(\Omega) \rightarrow V$ and a positive constant C_{inv} such that for all $v \in L^2(\Omega)$, it holds that $\pi \mathcal{Q}_H v = \pi v$ and $\|\mathcal{Q}_H v\|_{\bar{a}} \leq C_{\text{inv}} \|\pi v\|_{\bar{s}}$. Moreover, for each coarse element K_i , $\mathcal{Q}_H v|_{K_i}$ depends only on the data of v in K_i and vanishes on ∂K_i .*

The remainder of this section is dedicated to proving an error estimate for the multiscale solution, as stated in [Theorem 4.8](#) below. Before we prove the [Theorem 4.8](#), we need to prove Cea's lemma of the multiscale problem [\(3.12\)](#).

LEMMA 4.7 (Cea's Lemma). *If u is the real solution of [\(2.4\)](#) and u_{ms} is the multiscale solution of [\(3.12\)](#), there exists a $v_{\text{ms}} \in V_{\text{ms}}$, such that*

$$\|u - u_{\text{ms}}\|_{\bar{a}} \leq \frac{\alpha}{\beta_{\text{cem}}} \|u - v_{\text{ms}}\|_{\bar{a}},$$

where $\alpha = C_1 + C_*(1 + C_{\text{po}} H^{-1} \sqrt{\Lambda})$ and $\beta_{\text{cem}} > 0$ is a constant from the inf-sup condition of the multiscale problem [\(3.12\)](#).

Proof. We only need to check the ellipticity and continuity of the bilinear form \mathcal{B} over V , where $V = V_1 \oplus V_{\text{ms}}$. For the continuity of \mathcal{B} , for all $u, v \in V$, we have

$$\mathcal{B}(u, \mathcal{T}v) = \underbrace{a(u, \mathcal{T}v)}_{I_1} - \underbrace{k^2(u, \mathcal{T}v)}_{I_2},$$

and for the second term I_2 , we use the resolution condition (4.1) and (3.8)

$$\begin{aligned} |I_2| &\leq k^2 \mu_{\text{msh}}^{-1} H^2 \int_{\Omega} |c| \mu_{\text{msh}} H^{-2} |u| \cdot |\mathcal{T}v| \, dx \\ &\leq C_1 k^2 \mu_{\text{msh}}^{-1} H^2 \|u\|_{\bar{s}} \|v\|_{\bar{s}} \leq C_* \Lambda (\Lambda^{-1} \|u\|_{\bar{a}}^2 + \|\pi u\|_{\bar{s}}^2)^{1/2} (\Lambda^{-1} \|v\|_{\bar{a}}^2 + \|\pi v\|_{\bar{s}}^2)^{1/2}. \end{aligned}$$

Meanwhile, utilizing Poincaré inequality, we can see that

$$\|\pi u\|_{\bar{s}} \leq \|u\|_{\bar{s}} \leq C_{\text{po}} H^{-1} \|u\|_{\bar{a}}, \quad \|\pi v\|_{\bar{s}} \leq \|v\|_{\bar{s}} \leq C_{\text{po}} H^{-1} \|v\|_{\bar{a}}.$$

Then we can obtain

$$|\mathcal{B}(u, \mathcal{T}v)| \leq C_1 \|u\|_{\bar{a}} \|v\|_{\bar{a}} + C_* (1 + C_{\text{po}} H^{-1} \sqrt{\Lambda}) \|u\|_{\bar{a}} \|v\|_{\bar{a}} \leq \alpha \|u\|_{\bar{a}} \|v\|_{\bar{a}},$$

where $\alpha = C_1 + C_* (1 + C_{\text{po}} H^{-1} \sqrt{\Lambda})$ is a constant. Then for the ellipticity of \mathcal{B} , we need to prove the inf-sup condition of the multiscale problem (3.12), demonstrating that

$$\inf_{u_{\text{ms}} \in V_{\text{ms}}} \sup_{v_{\text{ms}} \in V_{\text{ms}}} \frac{\mathcal{B}(u_{\text{ms}}, v_{\text{ms}})}{\|u_{\text{ms}}\|_{\bar{a}} \|v_{\text{ms}}\|_{\bar{a}}} \geq \beta_{\text{cem}},$$

where β_{cem} is a positive constant. First, for any $u_{\text{ms}} \in V_{\text{ms}}$, we can find ψ such that $u \in V_{\text{ms}} = \hat{\mathcal{G}}^m \psi$. Then we choose $u_{\text{glo}} = \mathcal{G}^\infty \psi$. Based on the inf-sup condition of the global version (4.5), we can find $v_{\text{glo}} = \mathcal{G}^\infty \phi \in V_{\text{glo}}$, such that $\mathcal{B}(u_{\text{glo}}, v_{\text{glo}}) \geq \beta_{\text{glo}} \|u_{\text{glo}}\|_{\bar{a}} \|v_{\text{glo}}\|_{\bar{a}}$. If we define $v_{\text{ms}} = \hat{\mathcal{G}}^m \phi$, then we can obtain

$$\begin{aligned} \mathcal{B}(u_{\text{ms}}, v_{\text{ms}}) &= \mathcal{B}(u_{\text{glo}}, v_{\text{glo}}) + \mathcal{B}(u_{\text{glo}}, v_{\text{ms}} - v_{\text{glo}}) + \mathcal{B}(u_{\text{ms}} - u_{\text{glo}}, v_{\text{ms}}) \\ &\geq \beta_{\text{glo}} \|u_{\text{glo}}\|_{\bar{a}} \|v_{\text{glo}}\|_{\bar{a}} - \underbrace{\alpha \|u_{\text{glo}}\|_{\bar{a}} \|v_{\text{ms}} - v_{\text{glo}}\|_{\bar{a}}}_{I_1} - \underbrace{\alpha \|u_{\text{ms}} - u_{\text{glo}}\|_{\bar{a}} \|v_{\text{ms}}\|_{\bar{a}}}_{I_2}. \end{aligned}$$

For I_1 , we need to give the estimate of $\|v_{\text{ms}} - v_{\text{glo}}\|_{\bar{a}} = \|(\hat{\mathcal{G}}^m - \mathcal{G}^\infty)\phi\|_{\bar{a}}$. From **Theorem 4.5**, it shows that $\|(\mathcal{G}^m - \mathcal{G}^\infty)\phi\|_{\bar{a}}$ is bounded by $\|\pi\phi\|_{\bar{s}}$. Then, the remaining task is to obtain $\|\pi\phi\|_{\bar{s}}$ can be bounded by $\|\mathcal{G}^\infty\phi\|_{\bar{a}}$. It is not harmful to assume that $\phi \in V$ with $\|\phi\|_{\bar{a}} \leq C_{\text{inv}} \|\pi\phi\|_{\bar{s}}$ from **Lemma 4.6**. Taking $\mathcal{T}\phi$ as a test function in (4.3), we can obtain that

$$\mathcal{B}(\mathcal{G}^\infty\phi, \mathcal{T}\phi) + s(\pi\mathcal{G}^\infty\phi, \pi\mathcal{T}\phi) = s(\pi\phi, \pi\mathcal{T}\phi).$$

The estimate (3.6) says that

$$C_3 \|\pi\phi\|_{\bar{s}}^2 - C_4 \|\phi\|_{\bar{a}}^2 \leq s(\pi\phi, \pi\mathcal{T}\phi)$$

where $C_3 \rightarrow 1$ and $C_4 \rightarrow 0$ as $\Upsilon \rightarrow \infty$. Therefore, if Υ is large enough and $\Lambda^{-1} \leq 1$, we can show that

$$\begin{aligned} C_5 \|\pi\phi\|_{\bar{s}}^2 &\leq (C_3 - C_4 C_{\text{inv}}^2) \|\pi\phi\|_{\bar{s}}^2 \leq C_3 \|\pi\phi\|_{\bar{s}}^2 - C_4 \|\phi\|_{\bar{a}}^2 \\ &\leq s(\pi\phi, \pi\mathcal{T}\phi) \leq \alpha \|\mathcal{G}^\infty\phi\|_{\bar{a}} \|\phi\|_{\bar{a}} + \|\pi\mathcal{G}^\infty\phi\|_{\bar{s}} \|\pi\mathcal{T}\phi\|_{\bar{s}} \\ &\leq \alpha \|\mathcal{G}^\infty\phi\|_{\bar{a}} \|\phi\|_{\bar{a}} + C_1 \|\pi\mathcal{G}^\infty\phi\|_{\bar{s}} \|\phi\|_{\bar{s}} \\ &\leq \alpha \|\mathcal{G}^\infty\phi\|_{\bar{a}} \|\phi\|_{\bar{a}} + C_1 \|\pi\mathcal{G}^\infty\phi\|_{\bar{s}} \left(\Lambda^{-1} \|\phi\|_{\bar{a}}^2 + \|\pi\phi\|_{\bar{s}}^2 \right)^{1/2} \\ &\leq \sqrt{C_1^2 + \alpha^2} \left(\|\mathcal{G}^\infty\phi\|_{\bar{a}}^2 + \|\pi\mathcal{G}^\infty\phi\|_{\bar{s}}^2 \right)^{1/2} \left(\|\phi\|_{\bar{a}}^2 + \|\pi\phi\|_{\bar{s}}^2 \right)^{1/2} \end{aligned}$$

$$\leq \sqrt{C_1^2 + \alpha^2} \sqrt{1 + C_{\text{inv}}^2} \left(\|\mathcal{G}^\infty \phi\|_{\bar{a}}^2 + \|\pi \mathcal{G}^\infty \phi\|_{\bar{s}}^2 \right)^{1/2} \|\pi \phi\|_{\bar{s}}.$$

Finally, after using Poincaré inequality, we can see that

$$\|\pi \mathcal{G}^\infty \phi\|_{\bar{s}} \leq \|\mathcal{G}^\infty \phi\|_{\bar{s}} \leq C_{\text{po}} H^{-1} \|\mathcal{G}^\infty \phi\|_{\bar{a}}.$$

Then, $\|v_{\text{ms}} - v_{\text{glo}}\|_{\bar{a}} \leq C'_* H^{-1} \|\mathcal{G}^\infty \phi\|_{\bar{a}} = \eta \|v_{\text{glo}}\|_{\bar{a}}$, where $C'_* = \frac{\sqrt{C_1^2 + \alpha^2} \sqrt{1 + C_{\text{inv}}^2} \sqrt{2C_{\text{po}}}}{C_5}$. Following the techniques in I_1 for I_2 , we can obtain $\|u_{\text{ms}} - u_{\text{glo}}\|_{\bar{a}} \leq C'_* H^{-1} \|\mathcal{G}^\infty \psi\|_{\bar{a}} = \eta \|u_{\text{glo}}\|_{\bar{a}}$. Combining with all together, we can obtain the inf-sup condition

$$\begin{aligned} \mathcal{B}(u_{\text{ms}}, v_{\text{ms}}) &= \mathcal{B}(u_{\text{glo}}, v_{\text{glo}}) + \mathcal{B}(u_{\text{glo}}, v_{\text{ms}} - v_{\text{glo}}) + \mathcal{B}(u_{\text{ms}} - u_{\text{glo}}, v_{\text{ms}}) \\ &\geq \beta_{\text{glo}} \|u_{\text{glo}}\|_{\bar{a}} \|v_{\text{glo}}\|_{\bar{a}} - \underbrace{\alpha \|u_{\text{glo}}\|_{\bar{a}} \|v_{\text{ms}} - v_{\text{glo}}\|_{\bar{a}}}_{I_1} - \underbrace{\alpha \|u_{\text{ms}} - u_{\text{glo}}\|_{\bar{a}} \|v_{\text{ms}}\|_{\bar{a}}}_{I_2} \\ &\geq \beta_{\text{glo}} \|u_{\text{glo}}\|_{\bar{a}} \|v_{\text{glo}}\|_{\bar{a}} - \alpha C'_* H^{-1} \|u_{\text{glo}}\|_{\bar{a}} \|v_{\text{glo}}\|_{\bar{a}} - \alpha C'_* H^{-1} \|u_{\text{glo}}\|_{\bar{a}} \|v_{\text{ms}}\|_{\bar{a}} \\ &\geq \underbrace{(\beta_{\text{glo}}/4 - 9\alpha\eta/4 - 3\alpha\eta/2)}_{\beta_{\text{cem}}} \|u_{\text{ms}}\|_{\bar{a}} \|v_{\text{ms}}\|_{\bar{a}}, \end{aligned}$$

where the last inequality comes from the $1/2 \|v_{\text{ms}}\|_{\bar{a}} \leq \|v_{\text{glo}}\|_{\bar{a}} \leq 3/2 \|v_{\text{ms}}\|_{\bar{a}}$ and $1/2 \|u_{\text{ms}}\|_{\bar{a}} \leq \|u_{\text{glo}}\|_{\bar{a}} \leq 3/2 \|u_{\text{ms}}\|_{\bar{a}}$ by the smallness of η . Then we obtain the Cea's lemma, if u is the real solution of (2.4) and u_{ms} is the multiscale solution of (3.12), there exists a $v_{\text{ms}} \in V_{\text{ms}}$,

$$\begin{aligned} \beta_{\text{cem}} \|u - u_{\text{ms}}\|_{\bar{a}}^2 &\leq \mathcal{B}(u - u_{\text{ms}}, u - u_{\text{ms}}) = \mathcal{B}(u - u_{\text{ms}}, u - v_{\text{ms}}) + \mathcal{B}(u - u_{\text{ms}}, v_{\text{ms}} - u_{\text{ms}}) \\ &\leq \alpha \|u - u_{\text{ms}}\|_{\bar{a}} \|u - v_{\text{ms}}\|_{\bar{a}}. \quad \square \blacksquare \end{aligned}$$

THEOREM 4.8. *Under assumption II, there exists constants Υ, Λ^* such that for any $\Upsilon \geq \Upsilon'$ and $\Lambda \geq \Lambda^*$, the multiscale solution u_{ms} of (3.12) exists and is unique. Moreover, the following error estimate holds that for any $m \geq 1, 1 \leq i \leq N$,*

$$\|u - u_{\text{ms}}\|_{\bar{a}} \leq C_{\text{cem}} \left(\frac{k^{-1}}{\sqrt{\Lambda}} + H^{-2} (m+1)^{d/2} \theta^{(m-1)/2} \right) \|f\|_{\bar{s}-1},$$

where constant C_{cem} depends on $\Upsilon^{-1}, \beta_{\text{cem}}$, and $\theta < 1$ is the constant independent of k, m and H . In particular, if $m \geq 4|\log(H)|/|\log(\theta)|$, then we have optimal order convergence in H ; i.e., it holds that

$$\|u - u_{\text{ms}}\|_{\bar{a}} \leq C_{\text{cem}}^{-1}(k) \|f\|_{\bar{s}-1} \approx \mathcal{O}(H).$$

Proof. By using of Cea's Lemma in Lemma 4.7, we can obtain there exists an $v_{\text{ms}} \in V_{\text{ms}}$, such that

$$\begin{aligned} \|u - u_{\text{ms}}\|_{\bar{a}} &\leq \frac{\alpha}{\beta_{\text{cem}}} \|u - v_{\text{ms}}\|_{\bar{a}} \\ &\leq \frac{\alpha}{\beta_{\text{cem}}} \left(\underbrace{\|u - u_{\text{glo}}\|_{\bar{a}}}_{I_1} + \underbrace{\|u_{\text{glo}} - v_{\text{ms}}\|_{\bar{a}}}_{I_2} \right) \\ &\leq \frac{\alpha}{\beta_{\text{cem}}} \left(\frac{C_1 \|f\|_{\bar{s}-1}}{\sqrt{\Lambda}} + (c_0(\Lambda) C_{\text{ol}})^{1/2} C'_* H^{-2} (m+1)^{d/2} \theta^{(m-1)/2} \|f\|_{\bar{s}-1} \right) \end{aligned}$$

For I_1 , we utilize the global error estimate Theorem 4.2, and for the constant C_1 , we use the resolution condition (4.1) again to obtain the estimate that C_1 depends on

k^{-1} . For I_2 , we assume $u_{\text{glo}} = \mathcal{G}^\infty \psi$ and let $v_{\text{ms}} = \hat{\mathcal{G}}^m \psi$. After repeating the steps in Lemma 4.7, we can have

$$I_2 \leq (c_0(\Lambda)C_{\text{ol}})^{1/2} C'_* H^{-1} (m+1)^{d/2} \theta^{(m-1)/2} \|\mathcal{G}^\infty \psi\|_{\bar{a}},$$

where the estimate of $\|\mathcal{G}^\infty \psi\|_{\bar{a}}$ comes from the inf-sup condition of the global problem (4.4)

$$C_{\text{po}} H^{-1} \|w_{\text{glo}}\|_{\bar{a}} \|f\|_{\bar{s}-1} \geq \|f\|_{\bar{s}-1} \|w_{\text{glo}}\|_{\bar{s}} \geq (f, w_{\text{glo}}) = \mathcal{B}(u_{\text{glo}}, w_{\text{glo}}) \geq \beta_{\text{glo}} \|u_{\text{glo}}\|_{\bar{a}} \|w_{\text{glo}}\|_{\bar{a}}. \quad \blacksquare$$

5. Numerical experiments. We conduct numerical experiments on a square domain $\Omega = (0, 1) \times (0, 1)$. All numerical experiments are simulated by using the Python libraries NumPy and SciPy. The coefficient profile σ and c are represented by a 400×400 matrix/image, with each element corresponding to a constant value on a fine element \mathcal{K}_h . The reference solution, auxiliary spaces, and multiscale bases are all calculated on the fine mesh \mathcal{K}_h using the Q_1 finite element method with fine mesh 400×400 . We measure the convergence of the proposed method using both the relative energy error and the relative L^2 error which are defined:

$$\frac{\|e_h\|_{\bar{a}}}{\|u_h\|_{\bar{a}}} \quad \text{and} \quad \frac{\|e_h\|_{L^2(\Omega)}}{\|u_h\|_{L^2(\Omega)}},$$

where u_h is the reference solution calculated by the Q_1 FEM on \mathcal{K}_h or the nodal interpolation of the exact solution (if available), and e_h is the error between the reference solution and the numerical solution. For the coarse mesh sizes H , we consider coarse meshes to be \mathcal{K}_H : 20×20 , 40×40 , and 80×80 . For simplicity, we take μ as

$$\mu|_{K_i} = \mu_{\text{msh}} \text{diam}(K_i)^{-2} c|_{K_i} = 24H^{-2} c|_{K_i}$$

For all numerical experiments, as suggested in [24].

5.1. Flat interface model. We initially examine a flat interface model, where the coefficient variables in (2.1) are defined as follows:

$$(5.1) \quad \sigma = c = \begin{cases} 1, & y \geq 0.5 \\ -3, & \text{otherwise} \end{cases}.$$

Then we denote $\Omega^+ = (0, 1) \times (0.5, 1)$ and $\Omega^- = (0, 1) \times (0, 0.5)$. We set fixed values $(\sigma_*^+, -\sigma_*^-)$ to (σ^+, σ^-) , where both σ_*^+ and σ_*^- are positive values. In the subsequent simulation, we choose $\gamma = 0.5$, $\sigma_*^- = 3$, $\sigma_*^+ = 1$ from (5.1) and design the exact solution u as

$$u(x_1, x_2) = \begin{cases} -\sigma_*^- x_1 (x_1 - 1) x_2 (x_2 - 1) (x_2 - \gamma), & \text{in } \Omega^+, \\ \sigma_*^+ x_1 (x_1 - 1) x_2 (x_2 - 1) (x_2 - \gamma), & \text{in } \Omega^-, \end{cases}$$

which corresponds to a smooth source term f given by

$$f(x_1, x_2) = \sigma_*^- \sigma_*^+ \left(2x_2(x_2-1)(x_2-\gamma) + x_1(x_1-1)(6x_2-2(\gamma+1)) - k^2 x_1(x_1-1)x_2(x_2-1)(x_2-\gamma) \right). \quad \blacksquare$$

For the setting of the proposed multiscale method, we fix $k = 4$ and $l_* = 3$ indicating that we calculate the first three eigenfunctions and construct three multiscale bases for each coarse element. At the same time, we vary the oversampling layers m from 1 to 4.

Table 1: The relative errors in the energy norm (in the columns labelled with $\|\cdot\|_{\bar{a}}$) and in the L^2 norm (in the columns labelled with $\|\cdot\|_{L^2(\Omega)}$).

H	Q1		$m = 2$		$m = 3$		$m = 4$	
	$\ \cdot\ _{\bar{a}}$	$\ \cdot\ _{L^2(\Omega)}$						
$\frac{1}{20}$	3.393e-4	1.900e-4	6.150e-2	5.581e-3	2.604e-3	3.220e-5	1.082e-4	1.369e-6
$\frac{1}{40}$	8.582e-5	4.801e-5	2.839e-2	1.199e-3	1.140e-3	2.652e-5	5.660e-5	1.246e-6
$\frac{1}{80}$	2.152e-5	1.203e-5	1.265e-2	6.209e-4	4.980e-4	2.206e-5	1.713e-4	5.386e-6

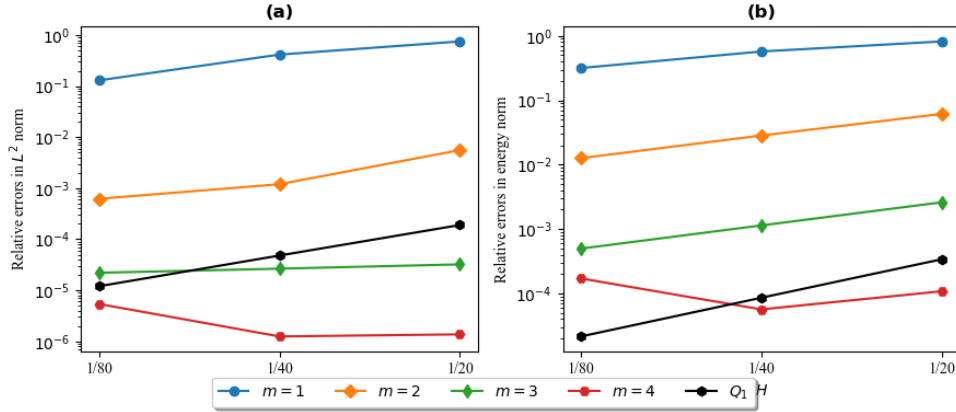


Fig. 2: The relative errors of the proposed method with different numbers of oversampling layers m and the Q_1 FEM are calculated w.r.t. the coarse mesh size H .

① We can observe from subplots (a) to (b) in Figure 2 that the convergence of the Q_1 FEM manifests a linear pattern w.r.t. H in the logarithmic scale, consistent with the theoretical expectation. ② In Table 1, we list the errors resulting from the refinement of the coarse mesh size alongside appropriately chosen oversampling layers. The first two columns represent the relative energy norm and the relative L^2 norm of the Q_1 FEM method. We can see that for $m = 4$, the proposed multiscale method exhibits higher accuracy than the Q_1 FEM. For the multiscale method, the relative energy norm is 0.0108% while the Q_1 FEM achieves 0.0339% when $H = 1/20$. ③ Figure 2 illustrates the errors of the CEM-GMsFEM for varying coarse sizes and oversampling layers. However, for the same m , the decaying error wrt H does not always hold, as depicted in subplots (a) and (b). This phenomenon differs from traditional FEMs but is common in CEM-GMsFEM. The reason is that the larger coarse mesh size H results in a larger oversampling domain, which can capture more local information, as stated in Theorem 4.8. ④ Additionally, we visualize the exact solution in Figure 3 (b)/(e), multiscale solutions in Figure 3 (a) and Q_1 FEM solutions in Figure 3 (d), further confirming the efficiency of our method.

5.2. Random inclusion model. In this subsection, we consider a random inclusion model that is utilized in several multiscale methods as a showcase of the capability of handling nonperiodic coefficient profiles [28, 21]. The subdomains Ω^+

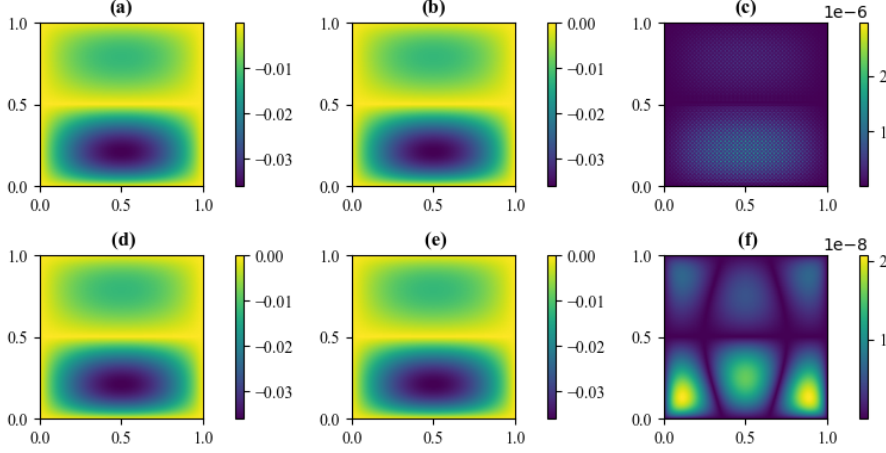


Fig. 3: **(a)** The solution approximated by the CEM-GMsFEM when we choose $H = 1/40$ and $m = 3$. **(d)** The solution approximated by the $Q1$ FEM when we choose $H = 1/40$. **(b)/(e)** The exact solution. **(c)** The difference of the solution approximated by CEM-GMsFEM with the exact solution. **(f)** The difference of solution approximated by $Q1$ -FEM with exact solution.

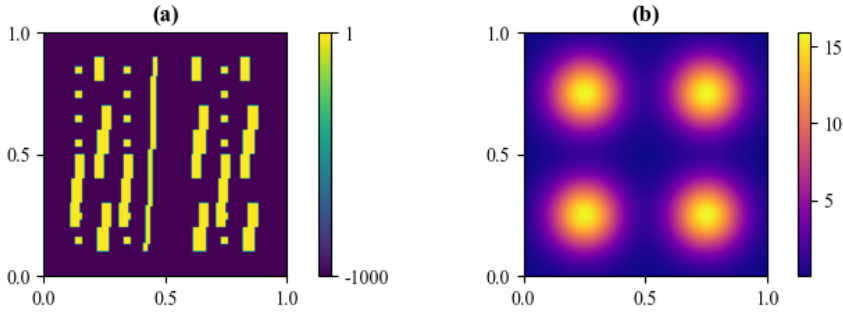


Fig. 4: **(a)** Coefficients with $(\sigma_*^+, \sigma_*^-) = (1, 10^3)$; **(b)** Source term based on Gaussian functions.

and Ω^- are demonstrated in [Figure 4-\(a\)](#), and σ is determined again by (σ_*^+, σ_*^-) . We consider $(\sigma_*^+, \sigma_*^-) = (1, 10^3)$ and set the source term f to be the following Gaussian function

$$f(x_1, x_2) = \frac{1}{\sigma\sqrt{2\pi}} \exp(-r^2/2\sigma^2)$$

where r is the distance from the point (x_1, x_2) to the center and σ is the standard deviation. The source function is depicted in [Figure 4-\(b\)](#). For the setting of the proposed multiscale method, we fix $k = 4$ and $l_* = 3$. [①](#) we outline the errors corresponding to the refinement of the coarse mesh size with the differently chosen oversampling layers in [Table 2](#). By decreasing the coarse mesh H , both the relative L^2

and the energy errors of the multiscale solution demonstrate convergence towards the fine grid solution, which is computed by the Q_1 FEM method. ② In Figure 5, there is an interesting phenomenon that the error does not decrease significantly for $H = 1/20$ or $H = 1/40$ when increasing m from 3 to 4. This is because the error is limited by the coarse mesh size H , and $m = 3$ is sufficient to achieve a good approximation. To visually underscore these observations, we plot the multiscale solution and the Q_1 FEM solution w.r.t. the coarse mesh size $H = 1/40$ and $m = 3$ in Figure 6. These two corresponding solutions are very close, with differences of only 1.60%. ③ we investigated how the number of basis functions affects the relative L^2 and the energy error norm with different oversampling layers for the specific case of $H = 1/20$. The findings, illustrated in Figure 7, indicate that an increase in the number of basis functions results in a noticeable reduction in both error norms. As we utilized more basis functions, we observed a significant enhancement in accuracy, as demonstrated by the decrease in the relative error and the energy error norm. The reason we choose $l_* = 3$ here is that the turning point appears between $l_* = 3$ and $l_* = 4$. This trend highlights the importance of selecting an appropriate number of basis functions to enhance the accuracy of multiscale methods.

Table 2: The relative errors in the energy norm (in the columns labelled with $\|\cdot\|_{\tilde{a}}$) and in the L^2 norm (in the columns labelled with $\|\cdot\|_{L^2(\Omega)}$).

H	$m = 1$		$m = 2$		$m = 3$		$m = 4$	
	$\ \cdot\ _{\tilde{a}}$	$\ \cdot\ _{L^2(\Omega)}$						
$\frac{1}{20}$	2.457e1	2.135e1	4.231e-2	2.340e-2	3.750e-2	2.357e-2	3.750e-2	2.357e-2
$\frac{1}{40}$	1.110	1.062	4.804e-2	1.475e-2	1.536e-2	5.488e-3	1.526e-2	5.485e-3
$\frac{1}{80}$	1.011	9.677e-1	1.385e-1	8.327e-2	5.810e-3	6.962e-4	3.971e-3	6.771e-4

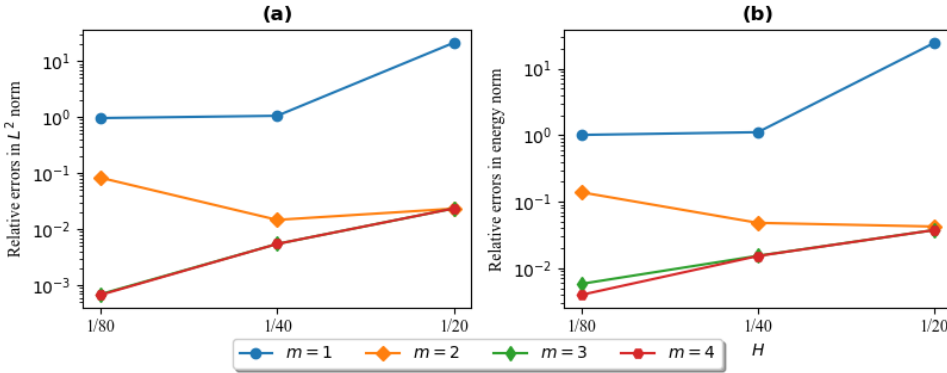


Fig. 5: The relative errors of the proposed method with different numbers of oversampling layers m and the Q_1 FEM are calculated w.r.t. the coarse mesh size H .

5.3. 2D negative-index materials. In this section, we provide an example demonstrating the interactions of Gaussian beams with 2D negative-index materials

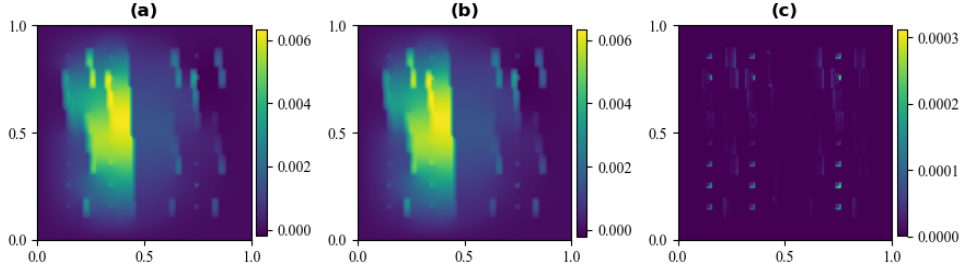


Fig. 6: **(a)** The solution approximated by the CEM-GMsFEM when we choose $H = 1/40$ and $m = 3$. **(b)** The solution approximated by the $Q1$ FEM when we choose $H = 1/40$.

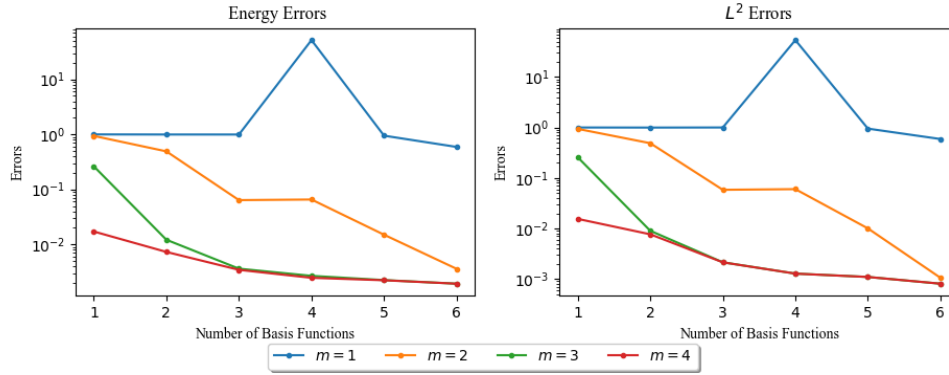


Fig. 7: The relative errors of the proposed method with different numbers of basis functions when $m = 3$ and $H = 1/20$.

[16, 30]. For the coefficients are defined as

$$\sigma = c = \begin{cases} 1, & \text{if } x < 11/24 \text{ or } x > 13/24 \\ -10, & \text{otherwise} \end{cases},$$

and depicted in **Figure 8-(a)**. Consequently, the subdomains Ω^+ and Ω^- are demonstrated in **Figure 8-(a)**, and σ is determined again by $(\sigma_*^+, \sigma_*^-) = (1, 10)$. The source wave is set as

$$f(x, y) = \exp(-((x - x_0)^2 + (y - y_0)^2)/(2\text{waist}^2)),$$

where beam center $(x_0, y_0) = (0, 0.5)$ and $\text{waist} = 0.05$, which is depicted in **Figure 8-(b)**. For the setting of the proposed multiscale method, we fix $k = 2\pi^2$ and $l_* = 3$.

① In **Table 3** and **Figure 9**, we compare the errors with different coarse mesh sizes and oversampling layers. Since the analytical solution is unavailable, we use the $Q1$ FEM solution as the reference solution. We observe the same phenomenon as shown in the second case. ② To illustrate the exotic properties of the materials

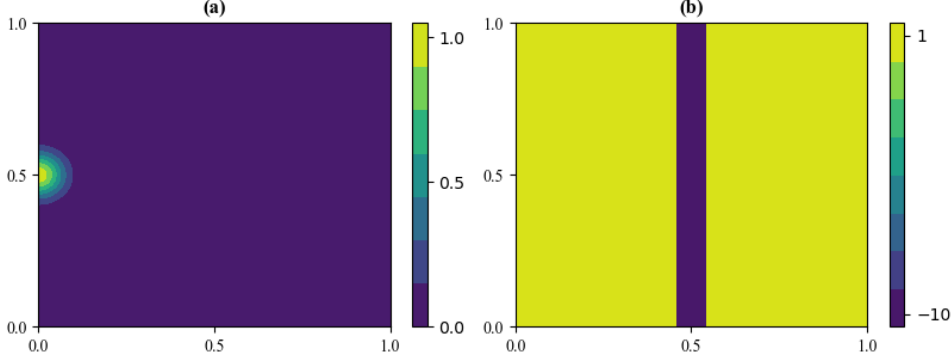


Fig. 8: **(a)** Gaussian Beam Source centered at $(0, 0.5)$. **(b)** The Negative index Materials.

Table 3: The relative errors in the energy norm (in the columns labelled with $\|\cdot\|_{\bar{a}}$) and in the L^2 norm (in the columns labelled with $\|\cdot\|_{L^2(\Omega)}$).

H	$m = 1$		$m = 2$		$m = 3$		$m = 4$	
	$\ \cdot\ _{\bar{a}}$	$\ \cdot\ _{L^2(\Omega)}$						
$\frac{1}{20}$	1.605e-1	6.037e-2	8.936e-3	7.528e-3	6.557e-3	5.328e-4	6.548e-3	5.318e-4
$\frac{1}{40}$	4.030e-1	2.142e-2	1.407e-2	7.699e-4	1.115e-3	4.604e-5	9.597e-4	3.837e-5
$\frac{1}{80}$	5.622e-1	5.702e-1	3.196e-2	2.486e-3	1.352e-3	3.032e-5	1.293e-4	2.639e-6

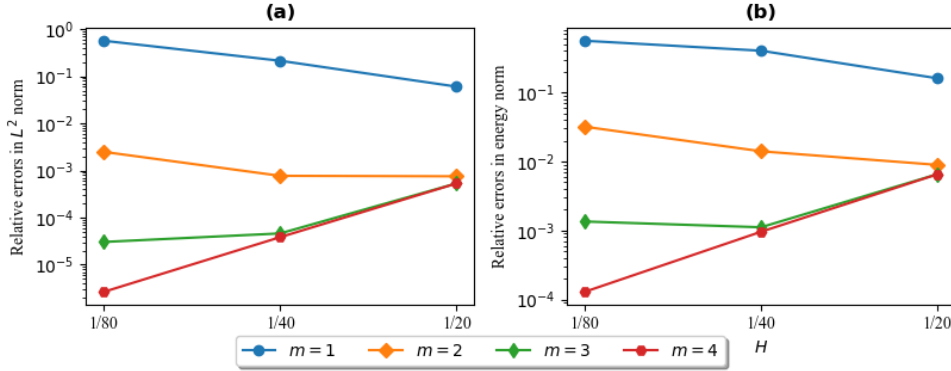


Fig. 9: The relative errors of the proposed method with different numbers of oversampling layers m and the Q_1 FEM are calculated w.r.t. the coarse mesh size H .

under discussion, the phenomenon of negative refraction is characterized in Figure 10. In this figure, the intensity values are represented with a color gradient, where the highest values are indicated in yellow and the lowest values are depicted in dark blue. Notably, as the beam propagates through the slab region $[1/3, 2/3]$, a vacuum area is

observed, which distinctly illustrates the refraction properties of the negative-index metamaterial (NIM) slab. This effect is further contextualized through the comparison in Figure 11, where we plot the solution within the non-signing domain when we choose $H = 1/40$ with $m = 3$. ③ This example serves as an in-silico simulation of metamaterials, particularly when a wave passes through the metamaterials, which demonstrates the efficiency of our newly proposed multiscale methods.

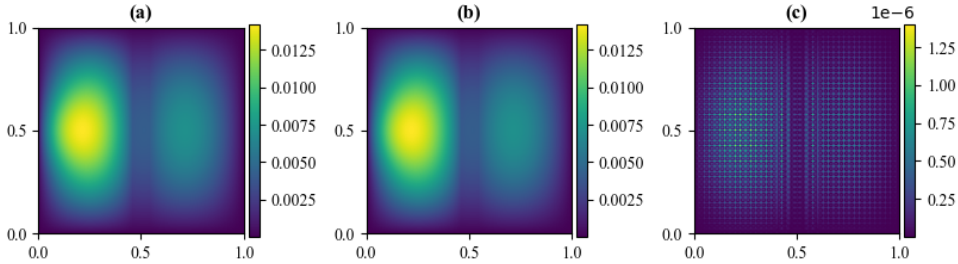


Fig. 10: (a) The solution approximated by the CEM-GMsFEM when we choose $H = 1/40$ and $m = 3$. (b) The solution approximated by the $Q1$ FEM when we choose $H = 1/40$.

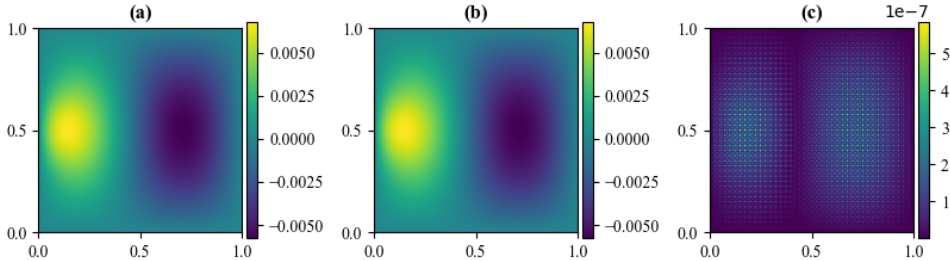


Fig. 11: (a) The solution approximated by the CEM-GMsFEM when we choose $H = 1/40$ and $m = 3$. (b) The solution approximated by the $Q1$ FEM when we choose $H = 1/40$.

6. Conclusion. We have proposed a multiscale computational method for solving conventional electromagnetic wave problems, utilizing the framework of CEM-GMsFEMs in the construction of multiscale basis functions. Due to a non-positive definite right-hand bilinear form, we have addressed this issue by replacing the coefficient with its absolute value in this step and explained that this modification complies with the T-coercivity theory and resolution condition. The final error estimates have been proved under several stringent assumptions, primarily related to the partitions of the coarse elements, the high-contrast values, the wavenumber and eigenvalues of the local spectral problem. The numerical experiments conducted have demonstrated the effectiveness of our methods. For the flat interface model with real solutions, our multiscale method demonstrates greater flexibility and accuracy when suitable

oversampling layers are selected, compared to the conventional $Q1$ FEM. In the second example, we test our method on a random inclusion model with a high-contrast coefficient. We find that choosing a small oversampling layer still yields good approximations while significantly reducing computational costs. Additionally, we discuss strategies for selecting the optimal number of multiscale basis functions to achieve the best performance. In the final example, we present a simulation of a wave passing through metamaterials, where we observe the intriguing phenomenon of a vacuum area being formed. This observation highlights the unique properties of metamaterials in manipulating wave behavior.

Multiscale bases are widely recognized as effective coarse spaces in the construction of multilevel domain decomposition or multigrid preconditioners [25, 26]. In this approach, the favourable property of multiscale computational methods, such as contrast robustness, can be leveraged to accelerate the numerical solvers. Considering the problem context, there exist two successive efforts: one for the sign-changing Laplace-type PDE and another for the Helmholtz-type PDE. The mathematical understanding of the former is well established, while the latter is still evolving. We emphasize that due to the non-coercive nature, employing the conventional multigrid preconditioner is not straightforward and can fail. One potential direction is to convert the original problem into a coercive one with an enriched space, and the multiscale can be utilized as a submodule in the entire solver. A satisfying answer to this question will significantly expand the computational scale in the current NIM simulations.

REFERENCES

- [1] L. C. ANNE-SOPHIE BONNET-BEN DHIA AND P. C. JR., *T-coercivity for the maxwell problem with sign-changing coefficients*, Communications in Partial Differential Equations, 39 (2014), pp. 1007–1031, <https://doi.org/10.1080/03605302.2014.892128>.
- [2] M. BARRÉ AND P. CIARLET JR., *The T-coercivity approach for mixed problems*. In press in Comptes Rendus Mathématique, 2023, <https://hal.science/hal-03820910>.
- [3] A. BONNET-BEN DHIA, P. CIARLET, AND C. ZWÖLF, *Time harmonic wave diffraction problems in materials with sign-shifting coefficients*, Journal of Computational and Applied Mathematics, 234 (2010), pp. 1912–1919, <https://doi.org/https://doi.org/10.1016/j.cam.2009.08.041>.
- [4] A.-S. BONNET-BENDHIA, L. CHESNEL, AND P. CIARLET JR., *T-coercivity for scalar interface problems between dielectrics and metamaterials*, ESAIM. Mathematical Modelling and Numerical Analysis, 46 (2012), pp. 1363–1387, <https://doi.org/10.1051/m2an/2012006>.
- [5] A.-S. BONNET-BENDHIA, L. CHESNEL, AND P. CIARLET JR., *T-coercivity for the Maxwell problem with sign-changing coefficients*, Communications in Partial Differential Equations, 39 (2014), pp. 1007–1031, <https://doi.org/10.1080/03605302.2014.892128>.
- [6] A.-S. BONNET-BENDHIA, L. CHESNEL, AND P. CIARLET JR., *Two-dimensional Maxwell's equations with sign-changing coefficients*, Applied Numerical Mathematics, 79 (2014), pp. 29–41, <https://doi.org/10.1016/j.apnum.2013.04.006>.
- [7] C. CARVALHO, L. CHESNEL, AND P. CIARLET JR., *Eigenvalue problems with sign-changing coefficients*, Comptes Rendus Mathématique, 355 (2017), pp. 671–675, <https://doi.org/10.1016/j.crma.2017.05.002>.
- [8] CHAUMONT-FRELET, THÉOPHILE AND VERFÜRTH, BARBARA, *A generalized finite element method for problems with sign-changing coefficients*, ESAIM: M2AN, 55 (2021), pp. 939–967, <https://doi.org/10.1051/m2an/2021007>.
- [9] E. CHUNG AND C. S. LEE, *A staggered discontinuous galerkin method for the convection–diffusion equation*, Journal of Numerical Mathematics, 20 (2012), pp. 1–32, <https://doi.org/doi:10.1515/jnum-2012-0001>.
- [10] E. T. CHUNG AND P. CIARLET, *A staggered discontinuous galerkin method for wave propagation in media with dielectrics and meta-materials*, Journal of Computational and Applied Mathematics, 239 (2013), pp. 189–207, <https://doi.org/https://doi.org/10.1016/j.cam.2012.09.033>.
- [11] E. T. CHUNG, Y. EFENDIEV, AND W. T. LEUNG, *Constraint energy minimizing generalized mul-*

- tiscale finite element method*, Computer Methods in Applied Mechanics and Engineering, 339 (2018), pp. 298–319, <https://doi.org/https://doi.org/10.1016/j.cma.2018.04.010>.
- [12] E. T. CHUNG, Y. EFENDIEV, AND G. LI, *An adaptive gmsfem for high-contrast flow problems*, Journal of Computational Physics, 273 (2014), pp. 54–76, <https://doi.org/https://doi.org/10.1016/j.jcp.2014.05.007>.
- [13] P. CIARLET JR., *T-coercivity: Application to the discretization of Helmholtz-like problems*, Computers & Mathematics with Applications, 64 (2012), pp. 22–34, <https://doi.org/10.1016/j.camwa.2012.02.034>.
- [14] T. Y. HOU AND X.-H. WU, *A multiscale finite element method for elliptic problems in composite materials and porous media*, Journal of Computational Physics, 134 (1997), pp. 169–189, <https://doi.org/https://doi.org/10.1006/jcph.1997.5682>.
- [15] H. H. KIM, E. T. CHUNG, AND C. S. LEE, *A staggered discontinuous galerkin method for the stokes system*, SIAM Journal on Numerical Analysis, 51 (2013), pp. 3327–3350, <https://doi.org/10.1137/120896037>.
- [16] J. LI, Y. CHEN, AND V. ELANDER, *Mathematical and numerical study of wave propagation in negative-index materials*, Computer Methods in Applied Mechanics and Engineering, 197 (2008), pp. 3976–3987, <https://doi.org/https://doi.org/10.1016/j.cma.2008.03.017>.
- [17] Z. LI, C. YE, AND E. T. CHUNG, *An iterative constraint energy minimizing generalized multiscale finite element method for contact problem*, Journal of Computational and Applied Mathematics, 461 (2025), p. 116398, <https://doi.org/https://doi.org/10.1016/j.cam.2024.116398>.
- [18] A. MÅLQVIST AND D. PETERSEIM, *Localization of elliptic multiscale problems*, Mathematics of Computation, 83 (2014), pp. 2583–2603, <https://doi.org/https://doi.org/10.1090/S0025-5718-2014-02868-8>.
- [19] J. PENDRY, A. HOLDEN, D. ROBBINS, AND W. STEWART, *Magnetism from conductors and enhanced nonlinear phenomena*, IEEE Transactions on Microwave Theory and Techniques, 47 (1999), pp. 2075–2084, <https://doi.org/10.1109/22.798002>.
- [20] J. B. PENDRY, *Negative refraction makes a perfect lens*, Physical review letters, 85 18 (2000), pp. 3966–9, <https://doi.org/https://doi.org/10.1103/physrevlett.85.3966>.
- [21] L. A. POVEDA, J. GALVIS, AND E. T. CHUNG, *A second-order exponential integration constraint energy minimizing generalized multiscale method for parabolic problems*, Journal of Computational Physics, 502 (2024), p. 112796, <https://doi.org/10.1016/j.jcp.2024.112796>.
- [22] R. A. SHELBY, D. R. SMITH, AND S. SCHULTZ, *Experimental verification of a negative index of refraction*, Science, 292 (2001), pp. 77 – 79, <https://doi.org/10.1126/science.1058847>.
- [23] V. G. VESELAGO, *The Electrodynamics of Substances with Simultaneously Negative Values of ϵ and μ* , Soviet Physics Uspekhi, 10 (1968), pp. 509–514, <https://doi.org/10.1070/PU1968v010n04ABEH003699>.
- [24] C. YE AND E. T. CHUNG, *Constraint energy minimizing generalized multiscale finite element method for inhomogeneous boundary value problems with high contrast coefficients*, Multiscale Modeling & Simulation. A SIAM Interdisciplinary Journal, 21 (2023), pp. 194–217, <https://doi.org/10.1137/21m1459113>.
- [25] C. YE, S. FU, E. T. CHUNG, AND J. HUANG, *A robust two-level overlapping preconditioner for darcy flow in high-contrast media*, SIAM Journal on Scientific Computing, 46 (2024), pp. A3151–A3176, <https://doi.org/10.1137/23M1558987>.
- [26] C. YE, S. FU, E. T. CHUNG, AND J. HUANG, *A highly parallelized multiscale preconditioner for darcy flow in high-contrast media*, Journal of Computational Physics, 522 (2025), p. 113603, <https://doi.org/https://doi.org/10.1016/j.jcp.2024.113603>.
- [27] C. YE, X. JIN, P. CIARLET JR, AND E. T. CHUNG, *Multiscale modeling for a class of high-contrast heterogeneous sign-changing problems*, arXiv:2407.17130, (2024), <https://doi.org/10.48550/arXiv.2407.17130>.
- [28] L. ZHAO AND E. T. CHUNG, *An analysis of the NLMC upscaling method for high contrast problems*, Journal of Computational and Applied Mathematics, 367 (2020), p. 112480, <https://doi.org/10.1016/j.cam.2019.112480>.
- [29] L. ZHAO AND E. T. CHUNG, *Constraint Energy Minimizing Generalized Multiscale Finite Element Method for Convection Diffusion Equation*, Multiscale Modeling & Simulation, 21 (2023), pp. 735–752, <https://doi.org/https://doi.org/10.1137/22M1487655>.
- [30] R. W. ZIOLKOWSKI, *Pulsed and cw gaussian beam interactions with double negative metamaterial slabs*, Optics Express, 11 (2003), pp. 662–681.